

## Chapter 1

# Tools for the rigorous proof of chaos and bifurcations

### 1.1 Introduction

In this section, we discuss the notion of *rigorous proof*. This notion is very problematic because there is no unified definition of a proof. However, there are several opinions as to what constitutes a proof, what is a rigorous proof, and more generally, what are the elements that constitute a proof. The so-called *four-color theorem* is an example of this problem since its “*proof*” is done by exhaustive computer testing of many individual cases and cannot easily be verified by hand. Such proofs are the subject of much controversy in the mathematical world. Some mathematicians think that the so-called *computer-assisted proofs* are valid and that the loss of the human verifiability of such proofs can be replaced by proving that the proof program itself is valid. Others disagree because of the non-verifiability of the different steps in the proof.

Hardy says in [Hardy (1999), pp. 15-16] that “*all physicists, and a good many quite respectable mathematicians, are contemptuous about proof. I have heard Professor Eddington, for example, maintain that proof, as pure mathematicians understand it, is really quite uninteresting and unimportant, and that no one who is really certain that he has found something good should waste his time looking for proof.... [This opinion], with which I am sure that almost all physicists agree at the bottom of their hearts, is one to which a mathematician ought to have some reply.*”

Hardy’s assertion given above was echoed by Feynman [Derbyshire (2004), pp. 291] who is reported to have commented, “*A great deal more is known than has been proved.*” However, we accept the following definitions:

**Definition 1.1.** (a) A proof is a rigorous mathematical argument which unequivocally demonstrates the truth of a given proposition.

(b) A proof is called rigorous if the validity of each step and the connections between the steps is explicitly made clear in such a way that the result follows with certainty.

In this book, the *rigorous proofs* that concern us are those dealing with the problem of locating orbits in a dynamical system, especially for the 2-D quadratic maps and the so-called *Chua's circuit* [Chua *et al.* (1986)]. These proofs can be classified into two types: The first is purely mathematical and use only a chain of logical steps that can be verified by hand, and the second is a mixture of mathematical tools and computer calculations. This latter type of rigorous proof is the one most used in the world of nonlinear sciences, especially for proving the existence and properties of different kinds of orbits, such as chaotic orbits, in a dynamical system because of their relevance to real applications. Note that the materials and tools presented here are independent of notation, applying equally to maps and to continuous-time systems.

Strange attractors can be classified into three principal classes [Anishchenko and Strelkova (1997), Chua *et al.* (1986), Plykin (2002)]: *hyperbolic*, *Lorenz-type*, and *quasi-attractors*. The hyperbolic attractors are the limit sets for which Smale's "axiom A" is satisfied and are structurally stable. Periodic orbits and homoclinic orbits are dense and are of the same saddle type, which is to say that they have the same index<sup>1</sup>. However, the Lorenz-type attractors are not structurally stable, although their homoclinic and heteroclinic orbits are structurally stable (hyperbolic), and no stable periodic orbits appear under small parameter variations, as for example in the Lorenz system [Lorenz (1963)]. The quasi-attractors are the limit sets enclosing periodic orbits of different topological types (for example, stable and saddle periodic orbits and structurally unstable orbits). For example, the attractors generated by Chua's circuit [Chua *et al.* (1986)] associated with saddle-focus homoclinic loops are quasi-attractors. Note that this type is more complex than the former two attractors and thus are not suitable for potential applications of chaos such as secure communications and signal masking. For further information about these types of chaotic attractors, see [Anishchenko and Strelkova (1997)].

In strange attractors of the hyperbolic type, all orbits in phase space are of the saddle type, and the invariant sets of trajectories approach the original one in forward or backward time, i.e., the stable and unstable manifolds intersect transversally. Generally, most known physical systems do not be-

---

<sup>1</sup>The same dimensions for their stable and unstable manifolds.

long to the class of systems with hyperbolic attractors [Anishchenko and Strelkova (1997)]. The type of chaos in them is characterized by chaotic trajectories and a set of stable orbits of large periods, not observable in computations because of their extremely small basins of attraction.

Hyperbolic strange attractors are robust (structurally stable) [Mira (1997)]. Thus, both from the point of view of fundamental studies and of applications, it would be interesting to find physical examples of hyperbolic chaos. For example, the Smale–Williams attractor [Kuznetsov and Seleznev (2006)] is constructed for a three-dimensional map, and the composed equations given by

$$\begin{cases} x' = -2\pi u + (h_1 + A_1 \cos 2\pi\tau/N)x - \frac{1}{3}x^3 \\ u' = 2\pi(x + \varepsilon_2 y \cos 2\pi\tau) \\ y' = -4\pi v + (h_2 - A_2 \cos 2\pi\tau/N)y - \frac{1}{3}y^3 \\ v' = 4\pi(y + \varepsilon_1 x^2) \end{cases} \quad (1.1)$$

are obtained by applying the so-called *equations of Kirchhoff* [Archibald (1988)], where the variables  $x$  and  $u$  are normalized voltages and currents in the  $LC$  circuit of the first self-oscillator ( $U_1$  and  $I_1$ , respectively), and  $y$  and  $v$  are normalized voltages and currents in the second oscillator ( $U_2$  and  $I_2$ ). Time is normalized to the period of oscillations of the first  $LC$  oscillator, and the parameters  $A_1$  and  $A_2$  determine the amplitude of the slow modulation of the parameter responsible for the Andronov–Hopf bifurcation in both self-oscillators. The parameters  $h_1$  and  $h_2$  determine a map of the mean value of this parameter from the bifurcation threshold, and  $\varepsilon_1$  and  $\varepsilon_2$  are coupling parameters. The system (1.1) has been constructed as a laboratory device [Kuznetsov and Seleznev (2006)], and an experimental and numerical solution were found. This example of a physical system with a hyperbolic chaotic attractor is of considerable significance since it opens the possibility for real applications. For further details, see [Kuznetsov and Seleznev (2006)].

The rigorous proof of chaos has a very long history because of the rich variety of dynamical systems, namely discrete and continuous-time, with and without known equations (dynamical system, time series, results of experiments, ...).

## 1.2 A chain of rigorous proof of chaos

In this section, we give as a main introduction for this book, many examples of dynamical systems with rigorous proofs of the chaos in their parameter

space. We concentrate on the examples of 2-D and 3-D real dynamical systems, i.e., systems with well known equations and well known domains of potential application.

As a Lorenz-type system, consider the original Lorenz system [Lorenz (1963)] given by

$$\begin{cases} x' = \sigma(y - x) \\ y' = rx - y - xz \\ z' = -bz + xy \end{cases} \quad (1.2)$$

These equations have proved to be very resistant to rigorous analysis and also present obstacles to numerical study. A very successful approach was taken in [Guckenheimer and Williams (1979), Afraimovich *et al.* (1982)] where they constructed so-called *geometric models* (these models are flows in three dimensions) for the behavior observed by Lorenz for which one can rigorously prove the existence of a robust attractor. Another approach through *rigorous numerics* [Hasting and Troy (1992), Hassard *et al.* (1994), Mischaikow and Mrozek (1995-1998)] showed that the equations exhibit a suspended Smale horseshoe. In particular, they have infinitely many closed solutions. A computer assisted proof of chaos for the Lorenz equations is given in [Tucker (1999), Stewart (2000), Franceschini *et al.* (1993), Galias and Zgliczynski (1998), Mischaikow and Mrozek (1995), Sparrow (1982)].

In [Tucker (1999)] a rigorous proof was provided that the geometric model does indeed give an accurate description of the dynamics of the Lorenz equations, i.e., it supports a strange attractor as conjectured by Lorenz in 1963. This conjecture was listed by Steven Smale as one of several challenging mathematical problems for the 21st century [Smale (1998-2000)]. Also a proof was given that the attractor is robust, i.e., it persists under small perturbations of the coefficients in the underlying differential equations. This proof is based on a combination of *normal form theory* and rigorous numerical computations. The robust chaotic Lorenz attractor is shown in Fig. 1.1. As a general result, it was proved in [Araujo *et al.* (2005)] that the so-called *singular-hyperbolic attractor* (or Lorenz-like attractor) of a three-dimensional flow is chaotic in two different strong senses: Firstly, the flow is expansive: if two points remain close for all times, possibly with time reparameterization, then their orbits coincide. Secondly, there exists a physical (or Sinai-Ruelle-Bowen) measure supported on the attractor whose ergodic basin covers a full Lebesgue (volume) measure subset of the topological basin of attraction. In particular, these results show that both the flow defined by the Lorenz equations and the geometric Lorenz flows are expansive.

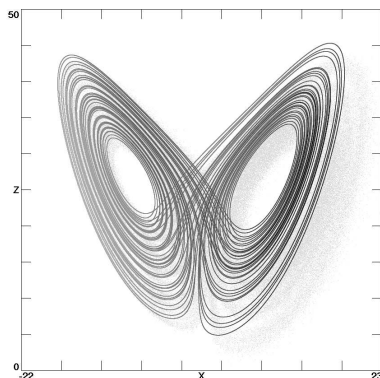


Fig. 1.1 The Lorenz chaotic attractor obtained from (1.2) for  $\sigma = 10, r = 28, b = \frac{8}{3}$  [Lorenz (1963)].

Another proof of the robustness of the Lorenz attractor is given in [Franceschini *et al.* (1993)] where the chaotic attractors of the Lorenz system for  $r = 28$  and  $r = 60$  were characterized in terms of their unstable periodic orbits and eigenvalues. While the Hausdorff dimension is approximated to very good accuracy in both cases, the topological entropy was computed in an exact sense only for  $r = 28$ . A general method for proving the robustness of chaos in a set of systems called  $C^1$ -robust transitive sets with singularities for flows on closed 3-manifolds is given in [Morales *et al.* (2004)]. The elements of the set  $C^1$  are partially hyperbolic with a volume-expanding central direction and are either attractors or repellers. In particular, any  $C^1$ -robust attractor with singularities for flows on closed 3-manifolds always has an invariant foliation whose leaves are forward contracted by the flow and has a positive Lyapunov exponent for every orbit, showing that any  $C^1$ -robust attractor resembles a geometric Lorenz attractor. A new topological invariant (Lorenz-manuscript) leading to the existence of an uncountable set of topologically different attractors is proposed in [Klinshpont *et al.* (2005)] where a new definition of the hyperbolic properties of the Lorenz system close to singular hyperbolicity is introduced, as well as a proof that small nonautonomous perturbations do not lead to the appearance of stable solutions.

Other than the Lorenz attractor, there are some works that focus on the proof of chaos and its robustness in 3-D continuous-time systems. For example the set  $C^1$  introduced in [Morales *et al.* (2004)], and a characterization of maximal transitive sets with singularities for generic  $C^1$ -vector

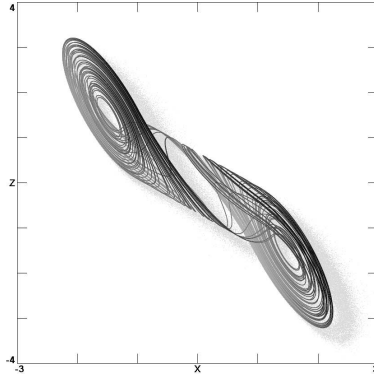


Fig. 1.2 The classic double-scroll attractor obtained from (1.3) for  $\alpha = 9.35$ ,  $\beta = 14.79$ ,  $m_0 = -\frac{1}{7}$ ,  $m_1 = \frac{2}{7}$  [Chua *et al.* (1986)].

fields on closed 3-manifolds in terms of homoclinic classes associated with a unique singularity is given and applied to some special cases.

However, no robust chaos occurs in quasi-attractor-type systems because the complexity of quasi-attractors is essentially due to the existence of structurally unstable homoclinic orbits in the system itself and in any system close to it. This results in a sensitivity of the attractor structure to small variations of the parameters of the generating dynamical equation, i.e., quasi-attractors are structurally unstable. Therefore, this type of system cannot generate robust chaotic attractors in the sense of this section [Mira (1997)]. Attractors generated by Chua's circuits [Chua *et al.* (1986)], given by

$$\begin{cases} x' = \alpha(y - h(x)) \\ y' = x - y + z \\ z' = -\beta y \end{cases} \quad (1.3)$$

where

$$h(x) = m_1 x + \frac{1}{2}(m_0 - m_1)(|x + 1| - |x - 1|) \quad (1.4)$$

are associated with saddle-focus homoclinic loops and are quasi-attractors. The corresponding, nonrobust, double-scroll attractor is shown in Fig. 1.2. Note that the chaos in Eq. (1.3) has been analytically proved by two independent methods [Chua *et al.* (1986), Matsumoto *et al.* (1988)] that are described in detail in Chapter 4 and constitute a major theme of this book.

### 1.3 Poincaré map technique

Let  $f : \mathbb{R} \times \Omega \longrightarrow \Omega$  be a continuous flow, where  $\Omega \subset \mathbb{R}^n$  is open. Let us consider the following  $n$ -dimensional continuous-time system given by

$$x' = f(t, x) \quad (1.5)$$

Let  $\varphi_t$  denote the corresponding flow of the system (1.5).

**Definition 1.2.** A map  $P$  is called a  $C^r$ -diffeomorphism if both  $P$  and  $P^{-1}$  its inverse are bijective and are  $r$  times continuously differentiable.

Let  $\gamma$  be a periodic orbit through a point  $p$ , and let  $U$  be an open and connected neighborhood of  $p$ . For any  $x \in \Omega$ , let  $I(x) = ]t_x^-, t_x^+[$  be an open interval in the real numbers. Then one has the following definitions:

**Definition 1.3.** (a) A positive semi-orbit through  $x$  is the set  $\gamma_x^+ = \{f(t, x), t \in ]0, t_x^+[\}$ , and a negative semi-orbit through  $x$  is the set  $\gamma_x^- = \{f(t, x), t \in ]t_x^-, 0[\}$ .

(b) A *Poincaré section* through a point  $p$  is a local differentiable and transversal section  $S$  of  $f$  through the point  $p$ .

Hence the Poincaré map is defined by the following:

**Definition 1.4.** A function  $P : U \longrightarrow S$  is called a Poincaré map for the orbit  $\gamma$  on the Poincaré section  $S$  through point  $p$  if:

- (1)  $P(p) = p$ .
- (2)  $P(U)$  is a neighborhood of  $p$  and  $P : U \rightarrow P(U)$  is a diffeomorphism.
- (3) For every point  $x$  in  $U$ , the positive semi-orbit of  $x$  intersects  $S$  for the first time at  $P(x)$ .

The relation between limit sets of the Poincaré map  $P$  and limit sets of the flow for the considered system (1.5) can be summarized as follows: A limit cycle of  $\varphi_t$  is a fixed point of  $P$ , and a period- $m$  closed orbit of  $P$  is a subharmonic solution (relative to the considered section  $S$ ) of  $\varphi_t$ . A chaotic orbit of  $P$  corresponds to a chaotic solution of  $\varphi_t$ . Also, a stable periodic point of  $P$  corresponds to a stable periodic orbit of  $\varphi_t$ , and an unstable periodic point of  $P$  corresponds to a saddle-type periodic orbit of  $\varphi_t$ .

#### 1.3.1 Characteristic multiplier

Assume that the system (1.5) has a limit cycle  $\Gamma$  and a Poincaré map  $P$  associated with this cycle at some arbitrary fixed point  $x^*$  located on this

cycle. Then the local behavior of the map  $P$  near  $x^*$  is determined by linearizing the map at  $x^*$ . Especially, the system

$$\delta x_{k+1} = DP(x^*) \delta x_k \quad (1.6)$$

where  $DP(x^*)$  is the Jacobian matrix of  $P$  evaluated at  $x = x^*$ , governs the evolution of the perturbation  $\delta x_0$  in a neighborhood of the fixed point  $x^*$ .

**Definition 1.5.** The eigenvalues of  $DP(x^*)$  are called characteristic multipliers of the periodic solution  $\Gamma$ .

The notion of characteristic multipliers was used to predict some routes to chaos in Chua's circuit as shown in Sec. 5.6.5.3.

### 1.3.2 The generalized Poincaré map

In this section, assume that the function  $f$  given in (1.5) is a continuous piecewise linear vector field. Let us denote by  $\Sigma_1, \dots, \Sigma_p$  the hyperplanes separating the linear regions  $U_i$  of  $f$ , so their union is the set  $\Omega$ . Let us denote by  $\varphi(t, x)$  the trajectory of the system starting at the point  $x$ .

**Definition 1.6.** The generalized Poincaré map  $H : \Omega \rightarrow \Omega$  is defined by  $H(x) = \varphi(\tau(x), x)$ , where  $\tau(x)$  is the time needed for the trajectory  $\varphi(t, x)$  to reach  $\Omega$ .

Note that the generalized Poincaré map  $H$  has the same properties given above for the map  $P$ . For evaluation of  $H$  in regions where  $H$  is continuous, one can use the analytical formulas for solutions of linear systems. In order to evaluate the generalized Poincaré map  $H$  on a box  $X \subset \Omega$ , we first find the return time for all points in  $X$ , i.e., the interval  $\{\tau(x), x \in X\} \subset \tau(X)$  and then use analytic solutions to compute  $\varphi(\tau(X), X)$ .  $H(X)$  is enclosed in the intersection of  $\varphi(\tau(X), X)$  with  $\Omega$ . The Jacobian of  $H$  at  $X$  can be expressed in terms of the return time  $\tau(x)$ , the start box  $X$ , and the image  $H(X)$ .

Some important properties of the Poincaré maps and their generalizations are as follows:

- (1) The Poincaré map  $P$  is sometimes called the *first recurrence map* because the method of analysis is to consider a periodic orbit with initial conditions on the Poincaré section  $S$  and observe the point at which this orbit first returns to the section  $S$ .

- (2) The Poincaré map is the intersection of a periodic orbit of the considered continuous-time system with the transversal Poincaré section<sup>2</sup>  $S$  in one dimension smaller than that of the original continuous dynamical system.
- (3) The map  $P$  is used to analyze the original system because it preserves many properties of the periodic and quasiperiodic orbits in the original continuous-time system.
- (4) There is no general method for constructing a Poincaré map. The majority of methods used here are numeric. In [Hénon (1982)], a method for accurately finding the intersections of a numerically integrated trajectory of a system of ordinary differential equations with a surface of section is given. A generalization of the *stopping procedure* described by Hénon is given in [Tucker (2002b)]. In [Tsuji and Ido (2002)], a computational method based on parallel computation of data tables and interpolation is given for calculating the Poincaré map. This method was successfully applied to the so-called *chaotic torus magnetic field line caused by the perturbation coil*. In [Fujisaka and Sato (1997)], a numerical method based on the Poincaré map, the second map constructed from the Poincaré map, and the topological degree is presented to compute the number and stability of fixed points of Poincaré maps of ordinary differential equations. The computation of the topological degree of the second map is equivalent to the calculation of the number of fixed points of the Poincaré map in a given domain of a Poincaré section. In some special cases, the Poincaré map was constructed rigorously by [Chua *et al.* (1986), Chua and Tichonicky (1991), Kuznetsov and Satayev (1994)] and references therein.
- (5) The Poincaré map  $P$  is not defined for points, trajectories of which never come back to the section  $S$  defining the map. Hence the image of a given set under  $P$  can be computed rigorously only if it is continuous on this set. Conversely, if the map  $P$  is well defined, this does not imply its continuity. One example of that is a point belonging to a stable manifold of an equilibrium of (1.5) where its trajectory converges to the fixed point and hence never comes back to the Poincaré plane  $S$ . A second example is where the map  $P$  is well defined but not continuous at points for which the flow is parallel to section  $S$  at this point or at the image  $P(S)$ .
- (6) If the map  $P$  is not continuous at a point, then in a close neighborhood

---

<sup>2</sup>This means that any periodic orbits starting on the subspace flow through  $S$  are not parallel to it.

of such a point rigorous evaluation of  $P$  becomes very difficult, the sets which have to be studied become smaller, and the computation time becomes longer. All these problems are circumvented if one knows the regions where the map  $P$  is not continuous.

### 1.3.3 Interval methods

In the interval Newton's method [Alefeld and Herzberger (1983), Neumaier (1990)], the existence of zeros of a function  $f$  in an  $n$ -dimensional interval  $X$  is established by evaluating the so-called *interval Newton operator*  $N(X)$  given by

$$N(X) = x_0 - (Df(X))^{-1} f(x_0) \quad (1.7)$$

where  $Df(X)$  is the interval matrix containing all Jacobian matrices of  $f$  for  $x \in X$  and  $x_0$  is an arbitrary point belonging to  $X$ . Hence the following theorem [Alefeld and Herzberger (1983), Neumaier (1990)] was obtained:

**Theorem 1.1.** *If  $N(X) \subset X$ , then there exists exactly one zero of  $f$  in  $X$ . If  $N(X) \cap X = \emptyset$ , then there are no zeros of  $f$  in  $X$ .*

Hence the interval Newton's method can be used to prove the existence and uniqueness of zeros. For computation of the expression  $(Df(X))^{-1} f(x_0)$ , one can use for example the Gaussian algorithm<sup>3</sup>.

Periodic orbits of a piecewise linear system can be rigorously studied by means of the interval Newton's method [Galias (2002a-2002b)]. The methods are based on the concept of a Poincaré map and the interval Newton's method to find regions where the generalized Poincaré map  $H$  is well defined and continuous and for locating all low-period cycles in this region. An example can be found in Sec. 4.8.1.

#### 1.3.3.1 Existence of periodic orbits

The existence of periodic solutions for continuous-time piecewise linear systems can be carried out using the generalized Poincaré map  $H$  associated with the continuous-time flow  $f$  given in (1.5). To prove the existence of a period- $m$  orbit of  $H$ , one applies the interval Newton's method to the map  $G : (\mathbb{R}^n)^m \rightarrow (\mathbb{R}^n)^m$  defined by

$$[G(z)]_k = x_{(k+1) \bmod m} - H(x_k), 0 < k < m \quad (1.8)$$

<sup>3</sup>The Gaussian elimination method (some elementary row operations) can be used to determine the solutions of linear equations, to find the rank of a matrix, and to calculate the inverse of an invertible square matrix [Lipschutz and Lipson (2001)].

where  $z = (x_0, \dots, x_{m-1})$ . We remark that  $G(z) = 0$  if and only if  $x_0$  is a fixed point of  $H^m$ . Note that this technique is limited to the subsets of  $\Omega$  where the Poincaré map  $H$  can be rigorously and effectively evaluated, and the problem of existence of periodic orbits for the system (1.5) is translated into the problem of existence of zeros of the higher-dimensional function  $G$ .

### 1.3.3.2 Interval arithmetic

Consider the following elements of the theory of *interval arithmetic*:

$$\begin{cases} X = [a, b] = \{x \in \mathbb{R} : a \leq x \leq b\} \\ V = (X_1, X_2, \dots, X_n) \\ X_1 \diamond X_2 = \{x = x_1 \diamond x_2 \in \mathbb{R}, : x_1 \in X_1, x_2 \in X_2\} \end{cases} \quad (1.9)$$

where:

$X$  : is an interval, i.e., a closed bounded set of real numbers.

$V$  : is called an  $n$ -dimensional interval vector, and it consists of  $n$  closed intervals  $X_i, i = 1, \dots, n$ .

$\diamond$  : is any of the following usual numeric operators:  $+$ ,  $-$ ,  $\times$ , and  $/$ , where all operations but division are defined for arbitrary intervals. For division, we assume that the interval  $X_2$  does not contain the number 0 because a real number  $a$  can be treated as a degenerate interval  $a = [a, a]$ .

Generally, all the steps of this method are summarized as follows [Galias (2001)]:

- (1) Reduce the continuous system (1.5) to the discrete one using the Poincaré map  $P$ .
- (2) Apply the interval Newton's operator  $G$  defined in (1.8).
- (3) Evaluate  $P(X)$  from Eq. (1.5) using direct integration by the Lohner method, which helps to reduce the *wrapping effect*<sup>4</sup> [Moore (1966), Lohner (1992)].
- (4) Find the image of  $P(X)$ , i.e., the intersection of  $\Omega$  and the trajectory computed by the rigorous integration procedure in step 3.
- (5) Find  $\dot{P}(X)$ , the Jacobian matrix of  $P(X)$  by solving the variational equation

$$\frac{dD}{dt} = \frac{\partial f}{\partial x}(x(t)) D \quad (1.10)$$

<sup>4</sup>The wrapping effect occurs when a solution set of a differential equation that is not a box (a parallelepiped with edges that are parallel to the axes of an orthogonal coordinate system) is enclosed or wrapped by a box on each integration step. A result of this wrapping phenomenon is that the computed bounds become unacceptably large.

where  $D(t, x_0) = \frac{\partial \varphi_t}{\partial x_0}(t, x_0)$  with the initial condition  $D(0, x_0) = I$ , the unit matrix.

- (6) Calculate the enclosure for the Jacobian matrix of  $P$  at  $x \in X$  using the formula:

$$P'(X) = \left( I - \frac{f(y)h^T}{h^T f(y)} \right) D \quad (1.11)$$

where:

$D$  is the enclosure for the solution of the variational equation

$$\{D(t, x), x \in X, t = \tau(x)\} \quad (1.12)$$

$h$  is a vector orthogonal to  $\Omega$  and  $y$  is the enclosure for the set  $\{P(x), x \in X\}$ .

- (7) Construct the trapping region<sup>5</sup>  $\tilde{\Gamma}$  for the Poincaré map  $P$ . Note that this region can be found by choosing a polygon enclosing trajectories of the Poincaré map  $P$  generated by the computer.
- (8) Cover the trapping region  $\tilde{\Gamma}$  by boxes of a specified size.
- (9) Apply a combination of the interval Newton's method and the generalized bisection technique to find all periodic orbits. This can be done in eight steps:

(9-1) Find the graph representation of the dynamics of the system<sup>6</sup>.

(9-2) Compute the image of each box.

(9-3) Find the set of admissible transitions (the so-called *transitions* represent edges of the directed graph) between boxes.

(9-4) Reduce the graph by removing vertices corresponding to boxes having no intersection with the invariant part of the trapping region. In this case, a box is removed if its image has no intersection with other boxes or if it has no intersection with images of all boxes.

(9-5) Repeat this procedure until no more boxes can be removed.

(9-6) Find all period- $m$  cycles in the resulting graph.

(9-7) Evaluate the interval operator for each period- $m$  cycle on the corresponding interval vector  $Z$ , and check what is the position of  $N(Z)$  with respect to  $Z$ , i.e., If  $N(Z) \subset Z$  then there exists exactly one period- $m$  cycle of  $f$  in  $Z$ . If  $N(Z) \cap Z = \emptyset$ , then there are no period- $m$  cycles of  $f$  in  $Z$ .

---

<sup>5</sup>A set  $\tilde{\Gamma}$  is said to be a trapping region, if it is positively invariant under the action of the map  $f$ , i.e.,  $f(x) \in \tilde{\Gamma}$  for all  $x \in \tilde{\Gamma}$ .

<sup>6</sup>For finding the graph representation of the dynamics of the system, the trapping region  $\tilde{\Gamma}$  must be covered by  $\epsilon$ -boxes of the form  $v = [k_1\epsilon_1, (k_1 + 1)\epsilon_1] \times [k_2\epsilon_2, (k_2 + 1)\epsilon_2]$  where  $k_i$  are integer numbers,  $\epsilon_i$  are fixed positive real numbers, and  $\epsilon = (\epsilon_1, \epsilon_2)$ .  $\epsilon$ -boxes define vertices, and admissible connections between boxes define edges of the graph.

(9-8) If the step (9-7) does not hold, then one option is to divide the interval vector  $Z$  into smaller parts and to evaluate the interval operator on each of them.

### 1.3.4 Mean value form

For evaluation of the Poincaré map  $H$  of a piecewise linear system, the so-called *mean value form* [Galias (2002b)] was used to eliminate some types of over-estimations of the resulting solutions set called the wrapping effect. Assume that in the linear regions  $\Sigma_k$  the system (1.5) has the form

$$x' = A_k(x - p_k) \quad (1.13)$$

Then its solution is given by

$$\varphi(t, x_0) = \exp(A_k t)(x_0 - p_k) + p_k \quad (1.14)$$

The following theorem was used to describe the method based on mean value form techniques:

**Theorem 1.2.** *Assume that  $H : \mathbb{R}^n \rightarrow \mathbb{R}^m$  is a  $C^1$  map. Then for all  $x, y \in \mathbb{R}^n$ , and for all  $i = 1, 2, \dots, m$ , there exists a point  $z_i$  in the interval  $\overline{xy}$  such that*

$$H_i(x) - H_i(y) = \sum_{j=1}^{j=m} \frac{\partial H_i}{\partial x_j}(z_i)(x_j - y_j) \quad (1.15)$$

Then, the mean value form techniques can be done in the following steps:

- (1) Take an interval vector  $X$ , fix a point  $y \in X$  as the center of  $X$ , and choose another point  $x \in X$ .
- (2) Apply Theorem 1.2, and deduce that there exists a point  $z_i \in X$  such that

$$\begin{cases} H_i(x) \in H_i(y) + \sum_{j=1}^{j=m} \frac{\partial H_i}{\partial x_j}(z_i)(x_j - y_j) \\ H(x) \in H(y) + DH(X)(x - y) \end{cases} \quad (1.16)$$

- (3) Deduce that

$$\{H(x) \in X\} \subset H(y) + DH(X)(x - y) \quad (1.17)$$

Clearly, more stringent computational results are obtained when the Poincaré map  $H$  is computed using Eq. (1.16). An example of the application of this method for Chua's circuit (1.3) is given in Sec. 4.8.1.

## 1.4 The method of fixed point index

The existence of the chaotic Hénon map [Hénon (1976)] was proved in [Zgliczynski (1997a)] using the method based on fixed point index. This method is described in Sec. 2.5.7, and it is done by introducing horseshoe-type mappings which are geometrically similar to Smale's horseshoes. The existence of chaotic dynamics and the semi-conjugacy introduced in Sec. 1.4.2 to the shift map on a finite number of symbols<sup>7</sup> are obtained for such mappings using the so-called *fixed point index*. This method is a purely topological one and does not require any assumptions concerning derivatives, and its assumptions can be rigorously verified by computer-assisted computations.

For a good presentation of this method, we need the following definitions:

Let  $(X, \rho)$  be a metric space. Let  $Z \subset X$  and  $x \in X$ . Let  $\text{int}(Z)$ ,  $\text{cl}(Z)$ ,  $\text{bd}(Z)$  denote the interior, the closure, and the boundary of the set  $Z$ , respectively. Let  $f : X \rightarrow X$  be any continuous map and  $N \subset X$ . Let  $G$  denote the class of pairs  $(f, Z)$ , such that  $Z$  is an open and bounded set and  $\text{cl}(Z) \subset X$ . Let  $f|_N$  denote the map obtained by restricting the domain of  $f$  to the set  $N$ .  $\text{Fix}f$  denotes the set of fixed points of  $f$ . Assume that  $f$  has no fixed points on  $\text{bd}(X)$ . The fixed point index theory introduced here using algebraic topology was developed in [Dold (1980)]. In particular, we use the property of the fixed point index which establishes the existence of a fixed point if the fixed point index is not zero. Here we give only the axiomatic definition:

**Definition 1.7.** The fixed point index is an integer valued function  $I : G \rightarrow \mathbb{Z}$  satisfying the following axioms:

- (1) If  $W$  is an open set such that  $\text{Fix}f \cap Z \subset W$ , then  $I(f, Z) = I(f, W)$ .
- (2) If  $f$  is constant, then  $I(f, Z) = 1$  if  $f(Z) \in Z$ , and  $I(f, Z) = 0$  if  $f(Z) \notin Z$ .
- (3) If  $Z$  is a sum of a finite number of open sets  $Z_i, i = 1, \dots, m$ , such that  $Z_i \cap Z_j \cap \text{Fix}f = \emptyset$  for  $i \neq j$ , then  $I(f, Z) = \sum_{i=1}^m I(f, Z_i)$ .
- (4) If  $f : X \rightarrow X, f' : X' \rightarrow X'$  are continuous maps and  $(f, Z), (f', Z')$  belong to the class  $G$ , then  $I((f, f'), Z \times Z') = I(f, Z)I(f', Z')$ .
- (5) if  $F_t : X \times [0, 1] \rightarrow \mathbb{R}^n$  is a homotopy,  $Z \subset X$ , and  $\text{Fix}f \cap \text{bd}(Z) = \emptyset$

<sup>7</sup>The class of TS-maps (the topological shifts), which includes as particular cases Smale's horseshoes [Smale (1967)], is used in this case.

for every  $t \in [0, 1]$ , then  $I(F_0, Z) = I(F_1, Z)$ .

Also, we need the definition of the maximal invariant part:

**Definition 1.8.** The maximal invariant part of  $N$  with respect to  $f$  is defined by

$$\text{Inv}(N, f) = \bigcap_{i \in \mathbb{Z}} f|_N^{-i}(Z). \quad (1.18)$$

For any set,  $P = \cup_k P_k = \cup_k [a_k, b_k] \times [c_k, d_k] \subset \mathbb{R}^2$ , where  $P_k$  are disjoint rectangles. Let us define the sets  $L(P)$ ,  $R(P)$ ,  $V(P)$ ,  $H(P)$  that are equal to the union of left vertical, right vertical, vertical, and horizontal edges in  $P$ , respectively:

$$\begin{cases} L(P) = \cup_k \{a_k\} \times [c_k, d_k] \\ R(P) = \cup_k \{b_k\} \times [c_k, d_k] \\ V(P) = L(P) \cup R(P) \\ H(P) = \cup_k ([a_k, b_k] \times \{c_k\} \cup [a_k, b_k] \times \{d_k\}) \end{cases} \quad (1.19)$$

Let us fix  $u, d \in \mathbb{R}$ ,  $u > d$  and a sequence  $a_{-1} = -\infty < a_0 < a_1 < \dots < a_{2K-2} < a_{2K-1} < a_{2K} = \infty$ , where  $a_i \in \mathbb{R}$ , for  $i = 0, 1, \dots, 2K - 1$ . Let:

$$\begin{cases} N_i = [a_{2i}, a_{2i+1}] \times [d, u], \text{ for } i = 0, \dots, K - 1 \\ E_i = [a_{2i-1}, a_{2i}] \times [d, u], \text{ for } i = 0, \dots, K \\ N = N_0 \cup N_1 \cup \dots \cup N_{K-1} \\ E = E_0 \cup E_1 \cup \dots \cup E_{K-1} \cup E_K \end{cases} \quad (1.20)$$

Then one has the following result [Zgliczynski (1997)]:

**Lemma 1.1.** *The sets  $E_i, N_i$  are contained in the horizontal strip  $(-\infty, \infty) \times [d, u]$  in the following order (if one compares  $x$ -coordinates):*

$$E_0 < N_0 < E_1 < N_1 < \dots < E_{K-1} < N_{K-1} < E_K \quad (1.21)$$

For  $i = 0, \dots, K$ , let us define the sets  $E'_i$  as follows:

$$\begin{cases} E_i = E'_i \cap (-\infty, \infty) \times [d, u] \\ cl(E'_i) \cap (N - V(N)) = \emptyset \\ cl(E'_i) \cap cl(E'_j) = \emptyset \text{ for } i \neq j \end{cases} \quad (1.22)$$

and suppose that there exist continuous homotopies  $h_i : [0, 1] \times E'_i \rightarrow E'_i$  such that

$$\begin{cases} h_i(0, p) = p \text{ for } p \in E'_i \\ h_i(1, p) \in E'_i \text{ for } p \in E'_i \\ h_i(t, p) = p \text{ for } p \in E'_i \text{ and } t \in [0, 1] \end{cases} \quad (1.23)$$

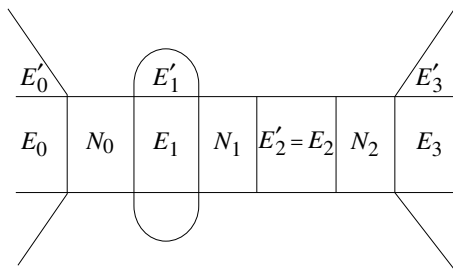


Fig. 1.3 An example of sets  $N_i$ ,  $E_i$ , and  $E'_i$  for  $K = 3$ .

Then one has the following result [Zgliczynski (1997b)]:

**Lemma 1.2.** (a) The set  $E'_i$  can be continuously deformed to the set of  $E_i$  without any intersection with the set  $N$ . (b) If

$$E' = E'_0 \cup E'_1 \cup \dots \cup E'_K \tag{1.24}$$

then

$$E'_i \cap N_j = \emptyset \text{ for } i, j = 0, 1, \dots, K - 1 \tag{1.25}$$

Fig. 1.3 presents a schematic drawing of the sets  $N_i$ ,  $E_i$ , and  $E'_i$  for  $K = 3$ .

**Definition 1.9.** Let the sets  $N_i$ ,  $E_i$ , and  $E'_i$  be as above. Let  $D$  be an open set such that  $N \subset D$  and the map  $f : D \rightarrow \mathbb{R}^2$  be continuous. We say that  $f$  is a TS-map (topological shift) (relative to the sets  $N, E, E'$ ) if there exist functions  $l, r : \{0, 1, \dots, K - 1\} \rightarrow \{0, 1, \dots, K\}$  such that the following conditions hold:

$$\begin{cases} f(L(N_i)) \subset E'_{l(i)} \\ f(R(N_i)) \subset E'_{r(i)} \\ f(N) \subset E' \cup N. \end{cases} \tag{1.26}$$

### 1.4.1 Periodic points of the TS-map

In this section, the periodic points of the TS-map  $f$  are characterized by periodic infinite sequences  $c = (c_i)_{i \in \mathbb{N}}$  of symbols  $0, 1, \dots, K - 1$  with the

---

<sup>8</sup>In this case, the set  $E_i$  is called the *deformation retract* of  $E'_i$ , where a deformation retraction is a map that captures the idea of continuously shrinking a space into a subspace.

property  $f^i(x) \in N_{c_i}$ , for  $i \in \mathbb{N}$ . Indeed, let

$$\begin{cases} \Sigma_K = \{0, 1, \dots, K - 1\}^{\mathbb{Z}} \\ \Sigma_K^+ = \{0, 1, \dots, K - 1\}^{\mathbb{N}} \end{cases} \tag{1.27}$$

Then (see also Sec. 2.5.7) [Zgliczynski (1997b)]:

**Lemma 1.3.** (a) *The sets  $\Sigma_K, \Sigma_K^+$  are topological spaces with a Tichonov topology.*

(b) *On  $\Sigma_K, \Sigma_K^+$ , the shift map  $\sigma$  is given by*

$$\sigma((c))_i = c_{i+1}. \tag{1.28}$$

Let  $A = (\alpha_{ij})$  be a  $K \times K$  matrix,  $\alpha_{ij} \in \mathbb{R}^+ \cup \{0\}$ ,  $i, j = 0, 1, \dots, K - 1$ . We define  $\Sigma_A \subset \Sigma_K$  and  $\Sigma_A^+ \subset \Sigma_K^+$  by

$$\begin{cases} \Sigma_A = \{c = (c_i)_{i \in \mathbb{Z}} : \alpha_{c_i c_{i+1}} > 0\} \\ \Sigma_A^+ = \{c = (c_i)_{i \in \mathbb{N}} : \alpha_{c_i c_{i+1}} > 0\} \end{cases} \tag{1.29}$$

Then one has the following result [Zgliczynski (1997b)]:

**Lemma 1.4.** *The sets  $\Sigma_A$  and  $\Sigma_A^+$  are invariant under  $\sigma$ .*

Let  $f$  be a  $TS$ -map. To relate the dynamics of  $f$  on  $Inv(N, f)$  with shift dynamics on  $\Sigma_K^+$ , we introduce the transition matrix of  $f$  denoted by  $A(f)$ . We define  $A(f)_{ij}$ , where  $i, j = 0, 1, \dots, K - 1$ :

$$A(f)_{ij} = \begin{cases} 1, & \text{if } E_{l(i)} < N_j < E_{r(i)} \text{ or } E_{l(i)} > N_j > E_{r(i)} \\ 0, & \text{otherwise.} \end{cases} \tag{1.30}$$

Then one has the following lemma [Zgliczynski (1997b)]:

**Lemma 1.5.** *If  $N_j$  lies between the images<sup>9</sup> of vertical edges of  $N_i$ , then  $A(f)_{ij} \neq 0$ , for all  $i, j = 0, 1, \dots, K - 1$ .*

### 1.4.2 Existence of semiconjugacy

For  $i \in \mathbb{N}$ , we define the map  $\pi_i : Inv(N, f) \rightarrow \{0, 1, \dots, K\}$  given by

$$\pi_i(x) = j \text{ if and only if } f^i(x) \in N_j. \tag{1.31}$$

Now we define the map  $\pi : Inv(N, f) \rightarrow \Sigma_K^+$  by

$$\pi(x) = (\pi_i(x))_{i \in \mathbb{N}}. \tag{1.32}$$

---

<sup>9</sup>In this case, one can deform the image by the homotopies  $h$  if necessary.

The map  $\pi$  assigns to the point  $x$  the indices of the rectangles  $N_i$  that its trajectory goes through.

Then one has [Zgliczynski (1997b)]:

**Lemma 1.6.** (a) *We have*

$$\pi \circ f = \sigma \circ \pi \tag{1.33}$$

(b) *If  $f$  is also a homeomorphism, then the definition of  $\pi_i$  can be extended to all integers, and the domain of  $\pi$  is  $\Sigma_K$ .*

Lemma 1.6(a) indicates the existence of a semi-conjugacy between  $f$  and  $\sigma$ , and this semi-conjugacy is not a sign of complicated dynamics because the set  $Inv(N, f)$  is finite or empty. However, the dynamics is complicated if the set  $\pi(Inv(N, f))$  is infinite as confirmed by the following theorem that gives the characterization of this set for TS-maps [Zgliczynski (1997)]:

**Theorem 1.3.** *Let  $f$  be a TS-map. Then  $\Sigma_{A(f)}^+ \subset \pi(Inv(N, f))$ . The preimage of any periodic sequence from  $\Sigma_{A(f)}^+$  contains periodic points of  $f$ . If we additionally suppose that  $f$  is a homeomorphism, then  $\Sigma_{A(f)} \subset \pi(Inv(N, f))$ .*

If we have the following definition:

**Definition 1.10.** Let  $N \subset \mathbb{R}^d$  be a compact set and  $f : N \rightarrow \mathbb{R}^d$  be a continuous map. The set  $N$  is called an isolating neighborhood if and only if

$$Inv(N, f) \subset Int(N). \tag{1.34}$$

Then the following theorem was proved in [Zgliczynski (1996)]:

**Theorem 1.4.** *Let  $N = \cup_{i=0}^{K-1} N_i$ , where  $N_i \subset \mathbb{R}^d$  are compact and disjoint. Let  $F : [0, 1] \times N \rightarrow \mathbb{R}^n$  be a continuous map such that  $N$  is an isolating neighborhood for  $F_\lambda$  for  $\lambda \in [0, 1]$ . Then for every finite sequence  $(\sigma_0, \sigma_1, \dots, \sigma_n) \in \{0, 1, \dots, K\}^{n+1}$ , the fixed point index*

$$I(F_\lambda^{n+1}, N_{\sigma_0} \cap F_\lambda^{-1}(N_{\sigma_1}) \cap \dots \cap F_\lambda^{-n}(N_{\sigma_n})) \tag{1.35}$$

*is defined and does not depend on  $\lambda$ .*

An application of this method to the Hénon map [Hénon (1976)] is given in Sec. 2.5.7.

## 1.5 Smale's horseshoe map

For defining the so-called *Smale's Horseshoe map*, we must define the unit square:

**Definition 1.11.** A unit square  $D$  with side lengths 1 is the one with coordinates  $(0, 0)$ ,  $(1, 0)$ ,  $(1, 1)$ ,  $(0, 1)$  in the real plane, or  $0, 1, 1 + i, i$  in the complex plane.

Thus Smale's horseshoe map  $f$  [Smale (1967), Cvitanović *et al.* (1988)] consists of the following sequence of operations as shown in Fig. 1.4 on the unit square  $D$  in blue and the following operations in red:

- (a) Stretch in the  $y$  direction by more than a factor of two.
- (b) Compress in the  $x$  direction by more than a factor of two.
- (c) Fold the resulting rectangle and fit it back onto the square, overlapping at the top and bottom, and not quite reaching the ends to the left and right and with a gap in the middle. Hence the action of  $f$  is defined through the composition of the three geometrical transformations defined above.
- (d) Endlessly repeating this procedure generates the horseshoe attractor with a Cantor set structure.

From Fig. 1.4, one sees that horseshoe maps cross the original square in a linear fashion, but in most applications, horseshoe maps are rarely so regular, although the behavior can be very similar.

Mathematically, the above actions can be translated as follows [Smale (1967)]:

- (a) Contract the square  $D$  by a factor of  $\lambda$  in the vertical direction, where  $0 < \lambda < \frac{1}{2}$ , such that  $D$  is mapped into the set  $[0, 1] \times [0, \lambda]$ .
- (b) Expand the rectangle obtained by a factor of  $\mu$  in the horizontal direction, where  $2 + \epsilon < \mu$ , and the set  $[0, 1] \times [0, \lambda]$  is mapped into the set  $[0, \mu] \times [0, \lambda]$  (the need for this  $\epsilon$  factor is explained in step 3).
- (c) Steps 1 and 2 produce a rectangle  $f(D)$  of dimensions  $\mu \times \lambda$ . This rectangle crosses the original square  $D$  in two sections after being bent as shown in Fig. 1.4. The  $\epsilon$  in step 2 indicates the extra length needed to create this bend as well as any extra on the other side of the square.
- (d) This process is then repeated, only using  $f(D)$  rather than the unit square. The  $n^{\text{th}}$  iteration of this process will be called  $f^k(D)$ ,  $k \in \mathbb{N}$ .

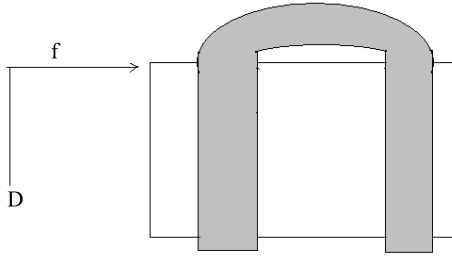


Fig. 1.4 Smale's horseshoe map  $f$  after a single iteration.

A picture showing some higher iterations of this process in Smale's horseshoe map  $f$  can be found in [Casselmann (2005)].

**1.5.1 Some basic properties of Smale's horseshoe map**

Before stating some important properties of Smale's horseshoe map  $f$ , we need the following definitions [Abraham and Marsden (1978)]:

Let  $f : \Omega \subset \mathbb{R}^n \rightarrow \mathbb{R}^n$  be a real function that defines a discrete map also called  $f$ .

**Definition 1.12.** (a) A point  $x$  is a nonwandering point for the map  $f$  if for every neighborhood  $U$  of  $x$  there is a  $k \geq 1$  such that  $f^k(U) \cap U$  is nonempty.

(b) The set of all nonwandering points is called the *nonwandering set* of  $f$ .

(c) An  $f$ -invariant subset  $\Lambda$  of  $\mathbb{R}^n$  satisfies  $f(\Lambda) \subset \Lambda$ .

(d) If  $f$  is a diffeomorphism defined on some compact smooth manifold  $\Omega \subset \mathbb{R}^n$ , an  $f$ -invariant subset  $\Lambda$  of  $\mathbb{R}^n$  is said to be hyperbolic if there exists a  $0 < \lambda_1 < 1$  and a  $c > 0$  such that

(d-1)  $T_\Lambda \Omega = E^s (+) E^u$ , where  $(+)$  means the direct algebraic sum.

(d-2)  $Df(x)E_x^s = E_{f(x)}^s$ , and  $Df(x)E_x^u = E_{f(x)}^u$  for each  $x \in \Lambda$ .

(d-3)  $\|Df^k v\| \leq c\lambda_1^k \|v\|$ , for each  $v \in E^s$  and  $k > 0$ .

(d-4)  $\|Df^{-k} v\| \leq c\lambda_1^{-k} \|v\|$ , for each  $v \in E^u$  and  $k > 0$ .

where  $E^s, E^u$  are the stable and unstable submanifolds of the map  $f$ , i.e., the two  $Df$ -invariant submanifolds, and  $E_x^s, E_x^u$  are the two  $Df(x)$ -invariant submanifolds.

When  $\Lambda = \Omega$ , then the diffeomorphism  $f$  is called an *Anosov diffeomorphism*.

**Definition 1.13.** The map  $f$  is an “*Axiom A*” diffeomorphism if

- (a) the nonwandering set  $\Omega(f)$  has a hyperbolic structure, and
- (b) the set of periodic points of  $f$  is dense in  $\Omega(f)$ , i.e.,  $\overline{Per(f)} = \Omega(f)$ , the closure is the nonwandering set itself.

Note that the “*Axiom A*” diffeomorphism serves as a model for the general behavior at a transverse homoclinic point where the stable and unstable manifolds of a periodic point intersect, and it plays a crucial role in the study of homoclinic bifurcations.

Then Smale’s horseshoe map  $f$  has the following properties given in the form of a lemma [Smale (1967)]:

**Lemma 1.7.** (a) *The horseshoe map  $f$  is a diffeomorphism defined from the unit square  $D$  of the plane into itself.*

(b) *The horseshoe map is one-to-one.*

(c) *The domain of  $f^{-1}$  is  $f(D)$ .*

(d) *The horseshoe map  $f$  is an *Axiom A* diffeomorphism.*

**Proof.** The proof of this lemma is based on the geometrical formations of horseshoes as shown in Fig. 1.4 and its repetitions.  $\square$

The presence of a horseshoe in a dynamical system implies the following important properties:

- (1) There is an infinite number of periodic orbits, especially those with arbitrarily long periods.
- (2) The number of periodic orbits grows exponentially with the period.
- (3) In any small neighborhood of any point of the fractal invariant set  $\Lambda$ , there is a point of a periodic orbit.

The proof of the above statements can be carried out using symbolic dynamics, and similar proofs have been given for Cantor’s set.

If one considers Smale’s horseshoe map as a set of topological operations, then the method for construction of an attractor of a dynamical system is Smale’s horseshoe map itself. This method consists of two operations. The first is the stretching which gives sensitivity to initial conditions, and the second is the folding which gives the attraction.

An example can be found in [Galias (1997b)]:

**Example 1.1.** Let  $\tilde{N}_0 = [-1, 1] \times [-1, -0.5]$ ,  $\tilde{N}_1 = [-1, 1] \times [0.5, 1]$ ,  $P_1 = [-1, 1] \times \mathbb{R}$ , be the smallest vertical stripe containing  $\tilde{N}_0$  and  $\tilde{N}_1$ ,  $M_- = [-1, 1] \times (-\infty, -1)$ ,  $M_0 = [-1, 1] \times (-0.5, 0.5)$ ,  $M_+ = [-1, 1] \times (1, \infty)$   $M_-$ ,

$M_0$ , and  $M_+$  are subsets of  $P_1$  lying below, between, and above  $\tilde{N}_0$  and  $\tilde{N}_1$ , respectively. Let  $N_{0D}$ ,  $N_{0U}$  be the lower and upper horizontal edges and  $N_{0L}$ ,  $N_{0R}$  be the left and right vertical edges of  $N_0$ , and similarly  $N_{1D}$ ,  $N_{1U}$ ,  $N_{1L}$ ,  $N_{1R}$  be the lower, upper, left, and right edges of  $\tilde{N}_1$ , respectively. Then Smale's horseshoe map is a map linear on  $\tilde{N}_0$  and  $\tilde{N}_1$  defined by

$$f(x, y) = \begin{cases} \left(\frac{1}{4}x - \frac{1}{2}, \pm 5\left(y + \frac{3}{4}\right)\right), & \text{if } (x, y) \in \tilde{N}_0 \\ \left(\frac{1}{4}x + \frac{1}{2}, \pm 5\left(y - \frac{3}{4}\right)\right), & \text{if } (x, y) \in \tilde{N}_1 \end{cases} \quad (1.36)$$

Note that the Jacobian of  $f^n$  is given by:

$$Df^n(x, y) = \begin{pmatrix} (0.25)^n & 0 \\ 0 & (\pm 5)^n \end{pmatrix} \quad (1.37)$$

The study of this example is done in Exercise 1.8 below.

### 1.5.2 Dynamics of the horseshoe map

The role of the horseshoe map is the reproduction of the chaotic dynamics of a flow in a small disk  $\Delta$  perpendicular to a period- $T$  orbit  $\Gamma$ . The important features in the dynamics of the map can be summarized as follows:

- (1) When the system evolves, some orbits diverge, and the points in this disk remain close to the given periodic orbit  $\Gamma$ , tracing out orbits that eventually intersect the disk once again.
- (2) The intersection of the disk  $\Delta$  and points in its neighborhood with the given period- $T$  orbit  $\Gamma$  comes back to itself every period  $T$ . When this neighborhood returns, its shape is transformed.
- (3) The points inside the disk  $\Delta$  consist of some that will leave the disk neighborhood and others that will continue to return.
- (4) The set of points that never leaves the neighborhood of the given period- $T$  orbit  $\Gamma$  forms a fractal.

The above features imply that Smale's horseshoe map consists of the iterated application of both  $f(D)$  and  $f^{-1}(D)$ .

Here some important results that can be found in [Smale (1967)]:

**Theorem 1.5.** (a) *The set  $\Pi_+ = \bigcap_{i=0}^{\infty} f^i(D)$  is an interval cross a Cantor-like set.*

(b) *The set  $\Pi_- = \bigcap_{i=0}^{\infty} f^{-i}(D)$  is a Cantor-like set cross an interval.*

(c) *The set  $\Pi = \Pi_+ \cap D \cap \Pi_-$  is a Cantor-like set cross a Cantor-like set.*

(d) If we consider the map  $f(D)$ , where  $f$  is the horseshoe map that contracts by  $\lambda$  and expands by  $\mu$ , where  $0 < \lambda < \frac{1}{2}$  and  $\mu > 2 + \epsilon$ , the Hausdorff dimension of  $\Pi$  is  $\log 2 \left( \frac{1}{\log \mu} - \frac{1}{\log \lambda} \right)$ .

(e) The limit set  $\Pi$  forms an uncountable, nowhere dense set (the interior of its closure is empty) in  $\mathbb{R}^2$ .

(f)  $f(D)$  is equivalent to the shift map in the symbolic space.

For more detail, see [Banks and Dragan (1994)].

These principal features give the idea that symbolic names can be given to all the orbits that remain in the neighborhood. If the initial disk  $\Delta$  can be divided into a small number of regions  $D_i$ ,  $i = 1, \dots, m$  and if one knows the sequence of points  $\{x_0, x_1, \dots\}$  in which the orbit visits these regions  $D_i$ , then the visitation sequence  $\hat{s} = \{\hat{s}_0; \hat{s}_1; \dots; \hat{s}_j; \dots\}$  composed of symbols  $\hat{s}_j = i$  if  $x_j = f^j(x_0) \in D_i$ ,  $i = 1, \dots, m$  of the orbits provide a symbolic representation of the dynamics, known as *symbolic dynamics* introduced in Sec. 1.5.3.

However, we have the following definition:

**Definition 1.14.** A dynamical system is chaotic in the sense of Smale if it has horseshoes of the Smale type.

Definition 1.14 with the so-called *shadowing lemma* [Stoffer and Palmer (1999)] was used to prove that the Hénon [Hénon (1976)] map is chaotic in the sense of Smale as shown in Sec. 2.5.6. Generally, there are no rigorous methods for finding Smale horseshoes in a dynamical system with relatively small dimension [Smale (1967), Banks and Dragan (1994)], but a few works are concerned with this topic. An example can be found in [Zgliczynski (1997b)] and is presented in Sec. 2.5.1.

### 1.5.3 Symbolic dynamics

Let  $S_m = \{0, 1, \dots, m - 1\}$  be the set of non-negative successive integers from 0 to  $m - 1$ . Let  $\Sigma_m$  be the collection of all bi-infinite sequences of  $S_m$  with their elements, i.e., every element  $s$  of  $\Sigma_m$  is of the form  $s = (\dots, s_{-n}, \dots, s_{-1}, s_0, s_1, \dots, s_n, \dots)$ ,  $s_i \in S_m$ . Let  $\bar{s} \in \Sigma_m$  be another sequence given by  $\bar{s} = (\dots, \bar{s}_{-n}, \dots, \bar{s}_{-1}, \bar{s}_0, \bar{s}_1, \dots, \bar{s}_n, \dots)$ ,  $\bar{s}_i \in S_m$ . Then:

**Definition 1.15.** The distance between  $s$  and  $\bar{s}$  is defined as

$$d(s, \bar{s}) = \sum_{-\infty}^{\infty} \frac{1}{2^{|i|}} \frac{|s_i - \bar{s}_i|}{1 + |s_i - \bar{s}_i|}. \quad (1.38)$$

Hence the set  $\Sigma_m$  with the distance defined as (1.38) is a metric space, and one has the following results proved in [Robinson (1995)]:

**Theorem 1.6.** *The space  $\Sigma_m$  is compact, totally disconnected, and perfect.*

A set having the three properties given in Theorem 1.6 is a Cantor set, which frequently appears in the characterization of the complex structure of an invariant set in a chaotic dynamical system. However, let an  $m$ -shift map  $\sigma : \Sigma_m \rightarrow \Sigma_m$  be defined by:

$$\sigma(s)_i = s_{i+1} \quad (1.39)$$

Then the map  $\sigma$  has the following properties proved in [Robinson (1995)]:

**Theorem 1.7.** (a)  $\sigma(\Sigma_m) = \Sigma_m$ , and  $\sigma$  is continuous.

(b) *The shift map  $\sigma$  as a dynamical system defined on  $\Sigma_m$  has the following properties:*

(b-1)  $\sigma$  has a countable infinity of periodic orbits consisting of orbits of all periods;

(b-2)  $\sigma$  has an uncountable infinity of nonperiodic orbits; and

(b-3)  $\sigma$  has a dense orbit.

The major result of statements (b) of Theorem 1.7 is that the dynamics generated by the shift map  $\sigma$  are sensitive to initial conditions, and therefore it is chaotic in the commonly accepted sense.

Now, let  $X$  be a separable metric space and  $f$  be a continuous map  $f : \tilde{Q} \rightarrow X$ , where  $\tilde{Q} \subset X$  is locally connected and compact.

**Assumption A** [Kennedy and York (2001)]. Suppose the following assumptions hold:

- A1. There exist two subsets of  $\tilde{Q}$ , denoted by  $\tilde{Q}_1$  and  $\tilde{Q}_2$ , respectively. The sets  $\tilde{Q}_1$  and  $\tilde{Q}_2$  are disjoint and compact,
- A2. Each connected component of  $\tilde{Q}$  intersects both  $\tilde{Q}_1$  and  $\tilde{Q}_2$ ,
- A3 The cross number  $m$  of  $\tilde{Q}$  with respect to  $f$  is not less than 2,

where the cross number  $m$  is defined as follows:

**Definition 1.16.** (a) A connection  $\tilde{\Gamma}$  for  $\tilde{Q}_1$  and  $\tilde{Q}_2$  is a compact subset of  $\tilde{Q}$  that intersects both  $\tilde{Q}_1$  and  $\tilde{Q}_2$ .

(b) A preconnection  $\tilde{\gamma}$  is a compact connected subset of  $\tilde{Q}$  for which  $f(\tilde{\gamma})$  is a connection.

(c) The cross number  $m$  is the largest number such that every connection contains at least  $m$  mutually disjoint preconnections.

Using these preliminaries, the following fundamental result was proved in [Kennedy and York (2001)]:

**Theorem 1.8.** *Let  $f$  be the map satisfying Assumption A. Then there exists a compact invariant set  $\tilde{Q}^I \subset \tilde{Q}$  for which  $f|_{\tilde{Q}^I}$  is semiconjugate to an  $m$ -shift map<sup>10</sup>.*

A more applicable version of the above result was given in [Yang and Tang (2004)] for piecewise continuous maps as follows:

**Theorem 1.9.** *Let  $\tilde{Q}$  be a compact subset of  $X$ , and  $f : \tilde{Q} \rightarrow X$  be a map satisfying the following conditions:*

(a) *There exist  $m$  mutually disjoint subsets  $D_1, \dots, D_m$  of  $\tilde{Q}$ , and the restriction of  $f$  to each  $D_i$ , i.e.,  $f|_{D_i}$  is continuous.*

(b)

$$\cup_{i=1}^m D_i \subset f(D_j), j = 1, 2, \dots, m \quad (1.40)$$

*Then there exists a compact invariant set  $K \subset \tilde{Q}$  such that  $f|_K$  is semi-conjugate to  $m$ -shift dynamics.*

Definition 1.16 can be generalized to an  $m$  domain  $D_1, \dots, D_{m-1}$  and  $D_m$  as follows:

**Definition 1.17.** Let  $\tilde{\gamma}$  be a compact subset of  $\tilde{Q}$  such that for each  $1 \leq i \leq m$ ;  $\tilde{\gamma}_i = \tilde{\gamma} \cap D_i$  is nonempty and compact. Then  $\tilde{\gamma}$  is called a connection with respect to  $D_1, \dots, D_{m-1}$  and  $D_m$ . Let  $\tilde{F}$  be a family of connections  $\tilde{\gamma}$ s with respect to  $D_1, \dots, D_{m-1}$  and  $D_m$  satisfying the following property:

$$\tilde{\gamma} \in \tilde{F} \implies f(\tilde{\gamma}_i) \subset \tilde{F} \quad (1.41)$$

Then  $\tilde{F}$  is said to be an  $f$ -connected family with respect to  $D_1, \dots, D_{m-1}$  and  $D_m$ .

Hence the following result was obtained and proved in [Yang and Tang (2004)]:

**Theorem 1.10.** *Suppose that there exists an  $f$ -connected family  $\tilde{F}$  with respect to  $D_1, \dots, D_{m-1}$  and  $D_m$ . Then there exists a compact invariant set  $K \subset \tilde{Q}$  such that  $f|_K$  is semi-conjugate to  $m$ -shift dynamics.*

A version of Theorem 1.8 was used in Sec. 4.8.2 to estimate the topological entropy of Chua's circuit in term of half-Poincaré maps.

---

<sup>10</sup>This holds if there exists a continuous and onto map  $h : \tilde{Q}^I \rightarrow \Sigma_m$  such that  $h \circ f = \sigma \circ h$ .

## 1.6 The Sil'nikov criterion for the existence of chaos

Homoclinic and heteroclinic orbits arise in the study of bifurcations and chaos, as well as in their applications to mechanics, biomathematics, and chemistry [Aulbach and Flockerzi (1989), Balmforth (1995), Feng (1998)]. In some cases, it is necessary to determine the nature or the type of chaotic behavior resulting from a dynamical system. One of the commonly used analytic criteria for proving chaos in autonomous systems is based on the work of Sil'nikov [Sil'nikov (1965-1970), Silva (2003)], whose role is similar to that of the Li-York lemma [Li and York (1975), Kennedy *et al.* (2001)] in the discrete case. The resulting chaos is called *horseshoe type* or *Sil'nikov chaos*. These horseshoes gives extremely complicated behavior typically observed in chaotic systems [Guckenheimer and Holmes (1983)] as shown in the previous section. A more detailed discussion of homoclinic bifurcations is given in Sec. 2.6.3 in connection with the Hénon map [Hénon (1976)].

### 1.6.1 Sil'nikov criterion for smooth systems

Consider the third-order autonomous system

$$x' = f(x) \tag{1.42}$$

where the vector field  $f : \mathbb{R}^3 \rightarrow \mathbb{R}^3$  belongs to class  $C^r$  ( $r \geq 1$ ),  $x \in \mathbb{R}^3$  is the state variable of the system, and  $t \in \mathbb{R}$  is the time. Suppose that  $f$  has at least one equilibrium point  $P$ .

**Definition 1.18.** (a) The point  $P$  is called a hyperbolic saddle focus for system (1.42) if the eigenvalues of the Jacobian  $A = Df(P)$  are  $\gamma, \rho + i\omega$ , where  $\rho, \gamma < 0$ , and  $\omega \neq 0$ .

(b) A homoclinic orbit  $\gamma(t)$  refers to a bounded trajectory of system (1.42) that is doubly asymptotic to an equilibrium point  $P$  of the system, i.e.,  $\lim_{t \rightarrow +\infty} \gamma(t) = \lim_{t \rightarrow -\infty} \gamma(t) = P$ .

(c) A heteroclinic orbit  $\delta(t)$  is similarly defined except that there are two distinct saddle foci  $P_1$  and  $P_2$  being connected by the orbit, one corresponding to the forward asymptotic time limit, and the other to the reverse asymptotic time limit, i.e.,  $\lim_{t \rightarrow +\infty} \delta(t) = P_1$ , and  $\lim_{t \rightarrow -\infty} \delta(t) = P_2$ .

The homoclinic and heteroclinic Sil'nikov method, namely, the Sil'nikov criterion for the existence of chaos, is summarized in the following theorem [Sil'nikov (1965-1970)]:

**Theorem 1.11.** *Assume the following:*

(i) The equilibrium point  $P$  is a saddle focus, and  $|\gamma| > |\rho|$ .

(ii) There exists a homoclinic orbit based at  $P$ . Then

(1) The Sil'nikov map, defined in a neighborhood of the homoclinic orbit of the system, possesses a countable number of Smale horseshoes in its discrete dynamics. (2) For any sufficiently small  $C^1$ -perturbation  $g$  of  $f$ , the perturbed system

$$x' = g(x) \quad (1.43)$$

has at least a finite number of Smale horseshoes in the discrete dynamics of the Sil'nikov map defined near the homoclinic orbit.

(3) Both the original system (1.42) and the perturbed system (1.43) exhibit horseshoe chaos.

Similarly, there is also a heteroclinic Sil'nikov theorem [Sil'nikov (1965-1970)] given by:

**Theorem 1.12.** *Suppose that two distinct equilibrium points, denoted by  $P_1$  and  $P_2$ , respectively, of system  $\dot{x} = f(x)$  are saddle foci whose characteristic values  $\gamma_k, \rho_k + i\omega_k$ , ( $k = 1, 2$ ) satisfy the following Sil'nikov inequalities:  $\rho_1\rho_2 > 0$ , or  $\gamma_1\gamma_2 > 0$ . Suppose also that there exists a heteroclinic orbit joining  $P_1$  and  $P_2$ . Then the system  $x' = f(x)$  has both Smale horseshoes and the horseshoe type of chaos.*

### 1.6.2 Sil'nikov criterion for continuous piecewise linear systems

Because we are interested in proving the existence of chaos in a continuous piecewise linear vector field, namely the so-called double-scroll system [Chua *et al.* (1986)], we must state a piecewise linear version [Silva (2003)] of Theorem 1.11 as follows:

**Theorem 1.13.** *Let  $\xi$  be a continuous piecewise linear vector field associated with a third-order autonomous system  $x' = \xi(x)$ , where  $x \in \mathbb{R}^3$ . Assume the origin is an equilibrium point with a pair of complex eigenvalues  $(\rho + i\omega, \rho < 0, \omega \neq 0)$  and a real eigenvalue  $\gamma > 0$  satisfying  $|\rho| < \gamma$ . If in addition,  $\xi$  has a homoclinic orbit through the origin, then  $\xi$  can be infinitesimally perturbed into a nearby vector field  $\xi'$  with a countable set of horseshoes.*

Using this version, [Chua *et al.* (1986)] proved that the double-scroll family studied in Chapter 4 is chaotic by showing that the conditions of

Sil'nikov's Theorem 1.13 is satisfied. In particular, for proving the existence of a homoclinic orbit, they proved that there exist parameters such that the trajectory along the unstable real eigenvector associated with the origin enters the complex stable eigenspace, and hence returns to the origin as shown in Sec. 4.5. The piecewise linear version of the heteroclinic Theorem 1.12 is posed as a challenge for the reader in Exercise 1.14.

## 1.7 The Marotto theorem

The Marotto theorem [Marotto (1978)], is best suited for predicting and analyzing discrete chaos in higher-dimensional difference equations because in practice, the homoclinic orbit or other techniques used for predicting chaos in dynamical systems are extremely difficult to compute, whereas the *snap-back repellors* are relatively easy, often needing only a small number of iterations.

First, consider the following one-dimensional discrete dynamical system:

$$x_{k+1} = f(x_k), x_k \in \mathbb{R}, k = 0, 1, 2, \dots \quad (1.44)$$

where the map  $f : \mathbb{R} \rightarrow \mathbb{R}$  is continuous. Then we have the following definition [Li and Yorke (1975)]:

**Definition 1.19.** A map  $f$  is chaotic (in the sense of Li and Yorke) if  $f$  has arbitrarily large periods and there exists an uncountable set  $S$ , called a scrambled set for  $f$ , such that for every  $x, y \in S$  and every periodic point  $z$  we have:

- (1)  $\lim_{k \rightarrow +\infty} \sup \|f^k(x) - f^k(y)\| > 0$
- (2)  $\lim_{k \rightarrow +\infty} \inf \|f^k(x) - f^k(y)\| = 0$
- (3)  $\lim_{k \rightarrow +\infty} \sup \|f^k(x) - f^k(z)\| > 0.$

If the map is  $n$ -dimensional, then we introduce the so-called *snap-back repeller* [Marotto (1978)] which is a generalization of the *scrambled set* given the Li-York definition of chaos in a one-dimensional discrete dynamical system. Indeed, consider the following nonlinear  $n$ -dimensional dynamical system:

$$X_{k+1} = f(X_k), X_k \in \mathbb{R}^n, k = 0, 1, 2, \dots \quad (1.45)$$

where the map  $f : \mathbb{R}^n \rightarrow \mathbb{R}^n$  is continuous. Denote by  $B_r(P)$  the closed ball in  $\mathbb{R}^n$  of radius  $r$  centered at a point  $P \in \mathbb{R}^n$ . Let  $f$  be differentiable in  $B_r(P)$ . The point  $P \in \mathbb{R}^n$  is an expanding fixed point of  $f$  in  $B_r(P)$  if

$f(P) = P$  and all eigenvalues of  $Df(X)$  exceed 1 in absolute value for all  $X \in B_r(P)$ . Then one has the following definition [Marotto (1978)]:

**Definition 1.20.** (Snap-back repellor): Assume that  $P$  is an expanding fixed point of  $f$  in  $B_r(P)$  for some  $r > 0$ . Then  $P$  is said to be a *snap-back repellor* of  $f$  if there exists a point  $P_0 \in B_r(P)$  with  $P_0 \neq P$  such that  $f^m(P_0) = P$  and the determinant  $|Df^m(P_0)| \neq 0$  for an integer  $m > 0$ .

Thus the Marotto theorem [Marotto (1978)] is given by:

**Theorem 1.14.** *If  $f$  is differentiable and has a snap-back repellor, the map (1.45) is chaotic in the sense of Li-Yorke, and*

(a) *there is a positive integer  $N$  such that for each integer  $p \geq N$ ,  $f$  has a point of period- $p$ , and*

(b) *there is a “scrambled set” of  $f$ , i.e., an uncountable set  $S$  containing no periodic points of  $f$  such that:*

(b-1)  $f(S) \subset S$ ,

(b-2) for every  $X_S, Y_S \in S$  with  $X_S \neq Y_S$ ,

$\lim_{k \rightarrow +\infty} \sup \|f^k(X_S) - f^k(Y_S)\| > 0$ ,

(b-3) for every  $X_S \in S$  and any periodic point  $Y_{per}$  of  $f$ ,

$\lim_{k \rightarrow +\infty} \sup \|f^k(X_S) - f^k(Y_{per})\| > 0$ ;

(c) *there is an uncountable subset  $S_0$  of  $S$  such that for every  $X_{S_0}, Y_{S_0} \in S_0$ :*

$\lim_{k \rightarrow +\infty} \sup \|f^k(X_{S_0}) - f^k(Y_{S_0})\| = 0$ .

Now consider the map

$$\begin{cases} x_{k+1} = f(x_k, by_k) \\ y_{k+1} = x_k \end{cases} \quad (1.46)$$

where  $f: \mathbb{R}^2 \rightarrow \mathbb{R}$  is differentiable. The map (1.46) can be reduced to the one-dimensional equation

$$x_{k+1} = f(x_k, 0) \quad (1.47)$$

when  $b$  is close to 0. Hence the following theorem was proved in [Marotto (1979a)]:

**Theorem 1.15.** *Suppose (1.47) has a snap-back repellor. Then (1.46) has a transversal homoclinic orbit for all  $|b| < \epsilon$  for some  $\epsilon > 0$ .*

Theorem 1.15 was used in [Marotto (1979b)] to prove that the Hénon map is chaotic as shown in Sec. 2.6.3.

## 1.8 The verified optimization technique

The verified optimization technique was introduced in [Tibor *et al.* (2006)], where a new version of this method was employed with some sufficient conditions to find chaotic regions for the Hénon map [Hénon (1976)]. The method is as follows:

- (1) Check the set theoretical conditions of a respective theorem in a reliable way by computer programs.
- (2) Introduce optimization problems that provide a model to locate chaotic regions.
- (3) Prove the correctness of the underlying checking algorithms and the optimization model.

The method given in [Zgliczynski (1997a)] works only with human interaction because of difficulties related to some mathematical relations. The actual method [Tibor *et al.* (2006)] finds chaotic regions automatically without any human assistance, where the techniques used are a combinations of interval arithmetic [Alefeld and Herzberger (1983), Neumaier (1990)] and *adaptive branch-and-bound subdivision* of the region of interest [Dellnitz and Junge (2002)].

### 1.8.1 The checking routine algorithm

For state this algorithm, we need the following inputs:

$\Upsilon$ : the respective mapping,

$\epsilon$ : the user set limit size of subintervals,

$Q'$ : the argument set to be proved,

$O'$ : the aimed set for which  $\Upsilon(Q') \subset O'$  is to be checked,

and the following definition:

**Definition 1.21.** A mapping  $F : I^n \rightarrow I^m$  is an inclusion mapping of the mapping  $f : \mathbb{R}^n \rightarrow \mathbb{R}^m$  if for  $\forall Y \in I^n$  and  $\forall y \in Y : f(y) \in F(Y)$ , where  $I$  stands for the set of all closed real intervals.

Hence the algorithm for an interval arithmetic based inclusion function [Ratschek and Rokne (1988)] is given by:

**Algorithm 1.1.** 1. Calculate the initial interval  $I$  that contains the regions of interest.

2. Push the initial interval onto the stack.

3. **while** the stack is nonempty,
4. Pop an interval  $v$  off the stack.
5. Calculate the width of  $v$ .
6. Determine the widest coordinate direction.
7. Calculate the transformed interval  $w = \Upsilon(v)$ .
8. **if**  $v \cap Q' \neq \emptyset$  and the condition  $w \subset O'$  does not hold, **then**
9. **if** the width of interval  $v$  is less than  $\epsilon$  **then**
10. **print** that the condition is hurt by  $v$  and **stop**,
11. **else** bisect  $v$  along the widest side:  $v = v_1 \cup v_2$  and
12. push the subintervals onto the stack
13. **endif**
14. **endif**
15. **end while**
16. **print** that the condition is proven and **stop**.

### 1.8.2 Efficacy of the checking routine algorithm

Note that each step in the checking routine algorithm needs some additional explanations in view of optimization theory [Dellnitz and Junge (2002)]. Here are some theorems that guarantee the efficacy of the checking routine algorithm [Tibor *et al.* (2006)]:

**Theorem 1.16.** *Assume that the underlying mapping  $\Upsilon$  is given by an inclusion mapping  $T$  and that the algorithm returns that the checked condition  $\Upsilon(Q') \subset O'$  is fulfilled. Then the checking routine algorithm generates a subdivision of the initial interval  $I$  around the search region in such a way that for all subintervals either,*

(i) *the subinterval does not contain a point of the argument region  $Q'$ ,*  
or

(ii) *the transformed subinterval is a subset of the respective set of the condition  $O'$ .*

**Theorem 1.17.** *Assume that the underlying mapping  $\Upsilon$  is given by an inclusion function  $T$  that has the zero convergence property,  $\epsilon = 0$ , and that  $T(Q') \subset O'$  holds. Then the checking routine algorithm concludes after a finite number of iteration steps that the condition of chaotic behavior is fulfilled.*

**Theorem 1.18.** *Assume that the underlying mapping  $\Upsilon$  is given by an inclusion function  $T$ ,  $\epsilon = 0$ , and there exist a point  $x \in Q'$  such that*

$T(x) \notin O'$ . Then the checking routine algorithm cannot conclude after a finite number of iteration steps whether the condition of chaotic behavior is fulfilled.

An example of the application of the checking routine algorithm can be found in Sec. 2.5.3.

The most crucial role of Smale's horseshoe is its relationship to the homoclinic tangency<sup>11</sup> discovered by Poincaré while investigating the three-body problem of celestial mechanics [Tuffillaro *et al.* (1987)].

**Definition 1.22.** (a) The invariant manifold of a map  $f$  is a set of points  $X$  such that  $f(X) \subset X$ <sup>12</sup>.

(b) Given a fixed point  $Y_0$  in the invariant manifold, the manifold  $Y$  is called stable if  $\forall y \in Y, \lim_{n \rightarrow \infty} f^n(y) \rightarrow Y_0$ . Similarly, a manifold is called unstable if  $\forall y \in Y, \lim_{n \rightarrow \infty} f^{-n}(y) \rightarrow Y_0$ .

(c) A fixed point is hyperbolic if it is the intersection of one or more stable manifolds and one or more unstable manifolds.

(c) A homoclinic point is a point  $x$ , different from a fixed point, that lies on both a stable manifold and an unstable manifold of the same fixed point  $Q$ .

**Theorem 1.19.** (Poincaré, 1890). *If there exists a single homoclinic point on a stable and an unstable invariant manifold corresponding to a particular hyperbolic fixed point, then there exist an infinite number of homoclinic points on the same invariant manifolds.*

**Proof.** The proof is done by induction on the number of homoclinic points. Assume that there exist  $n$  homoclinic points for these invariant manifolds. Let  $W^s(Q)$  be the stable manifold and  $W^u(Q)$  be the unstable manifold, and let  $x$  be the homoclinic point farthest from the fixed point  $Q$  along the unstable manifold  $W^u(Q)$ . Since  $W^s(Q)$  and  $W^u(Q)$  are invariant manifolds,  $f(x) \in W^s(Q) \cap W^u(Q)$ . Thus  $f(x)$  is either a homoclinic point or the fixed point  $Q$ . Since  $f$  takes a point on the unstable manifold  $W^u(Q)$  away from the fixed point  $Q$ , then  $f(x)$  cannot be the fixed point. Thus it is a homoclinic point. For the same reason, it is not one of the  $n$  considered homoclinic points. Thus there exist  $n + 1$  homoclinic points.

<sup>11</sup>The homoclinic tangency is the tangled intersection of such invariant manifolds with a homoclinic point as shown in Fig. 1.5.

<sup>12</sup>Of course every fixed point, with the exception of centers, will be an element of some invariant manifold.

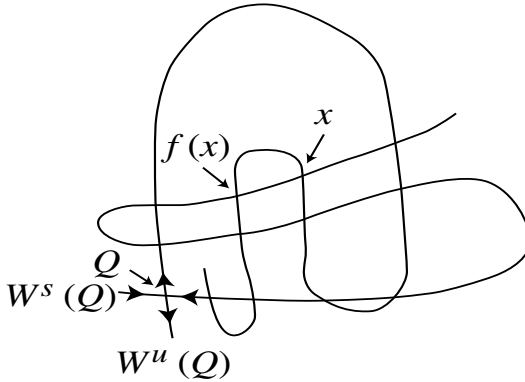


Fig. 1.5 Part of a homoclinic tangency:  $Q$  is the hyperbolic fixed point,  $W^s(Q), W^u(Q)$  are the stable and unstable manifolds, respectively,  $x$  is a homoclinic point, and thus  $f(x)$  is also a homoclinic point.

Therefore, the number of homoclinic points on the corresponding invariant manifolds is infinite.  $\square$

Hence the basic theorem about the rigorous proof of chaos for a dynamical system  $f : \mathbb{R}^n \rightarrow \mathbb{R}^n$  was proved by [Smale (1967)]:

**Theorem 1.20.** *If  $f$  is a diffeomorphism and has a transversal homoclinic point, then there exists a Cantor set  $\Lambda \subset \mathbb{R}^n$  in which  $f^m$  is topologically equivalent to the shift automorphism for some  $m$ .*

The existence of the shift automorphism implies the existence of a dense set of periodic orbits and an uncountably infinite collection of asymptotically aperiodic points of the map  $f$  within the set  $\Lambda$ .

It is not difficult to show that the homoclinic tangency has the same topological structure as the horseshoe map [Weisstein (2002)] using some geometrical illustrations.

## 1.9 Shadowing lemma

It is well known that there are rounding errors at every step when calculating a trajectory of a dynamical system. If the dynamical system has a chaotic attractor, these errors will grow exponentially, and the resulting orbit will differ wildly from the exact one. The so-called, *shadowing lemma* introduced in [Palmer (1988)] eliminates this problem and ensures

that, under quite general conditions, there is a trajectory of the true system starting from a slightly perturbed initial state that remains in the vicinity of the computed one for all time.

The general Shadowing lemma can be applied on an arbitrary Riemannian manifold as follows:

**Theorem 1.21.** *Let  $\Omega$  be a Riemannian manifold,  $f : \Omega \rightarrow \Omega$ , a diffeomorphism, and let  $\tilde{\Lambda} \subset \Omega$  be a compact hyperbolic set for  $f$ . Then there is a neighborhood  $U$  of  $\tilde{\Lambda}$  such that for every  $\delta > 0$  there is an  $\epsilon > 0$  for which every  $\epsilon$ -orbit in  $U$  is  $\delta$ -shadowed by an orbit of  $f$ .*

*Moreover, there is a  $\delta_0 > 0$  such that, if  $\delta < \delta_0$  and if the pseudo-orbit is bi-infinite, then the shadowing orbit is unique, and if  $\tilde{\Lambda}$  has a local product structure, then the shadowing orbit is in  $\tilde{\Lambda}$ .*

Generally, the standard use of the shadowing lemma in dynamical systems theory is to prove density of periodic points, and because our interest is the study of the shadowing lemma in real systems, namely 2-D quadratic maps and the Chua systems as an example of ODE dynamics, then  $\Omega = \mathbb{R}^n$ ,  $n = 2, 3$ , and  $M$  is a Riemannian manifold. However, the following definitions help in understanding Theorem 1.21:

**Definition 1.23.** (a) An  $\epsilon$ -pseudo-orbit for  $f$  is a sequence  $\{x_n, n \in \mathbb{Z}\}$ , such that  $|x_n - f(x_{n-1})| < \epsilon$  for all  $n \in \mathbb{Z}$ .

(b) A sequence  $\{x_k, k \in \mathbb{Z}\}$  is said to be an  $\epsilon$ -pseudo-periodic-orbit with period- $N$  of  $f$  if  $|x_{k+1} - f(x_k)| < \epsilon$  and  $x_{k+N} = x_k$  for  $k \in \mathbb{Z}$ <sup>13</sup>.

(c) Let  $\{x_k, k \in \mathbb{Z}\}$  and  $\{y_k, k \in \mathbb{Z}\}$  be two  $\epsilon$ -pseudo-periodic-orbits. A sequence  $\{z_k, k \in \mathbb{Z}\}$  is said to be an  $\epsilon$ -pseudo-connecting-orbit connecting  $\{x_k, k \in \mathbb{Z}\}$  to  $\{y_k, k \in \mathbb{Z}\}$  if

(i)  $|z_{k+1} - f(z_k)| < \epsilon$ , for  $k \in \mathbb{Z}$ .

(ii)  $z_k = x_k$  for  $k \leq p$ , and  $z_k = y_k$  for  $k \geq q$  for some integers  $p < q$ .

(d) In the case  $\{x_k, k \in \mathbb{Z}\} = \{y_{k+\tau}, k \in \mathbb{Z}\}$  for some  $\tau$ , the  $\epsilon$ -pseudo-connecting-orbit  $\{z_k, k \in \mathbb{Z}\}$  is called an  $\epsilon$ -pseudo-homoclinic-orbit.

(e) A hyperbolic set  $\tilde{\Lambda}$  is a compact invariant set of a diffeomorphism  $f$  such that the tangent space at every  $x \in \tilde{\Lambda}$  admits an invariant splitting that satisfies the contraction and expansion conditions given in Definition 1.12(d).

---

<sup>13</sup>More precisely, a periodic orbit  $\{x_n, n \in \mathbb{Z}\}$  is a finite set of points.

### 1.9.1 Shadowing lemmas for ODE systems and discrete mappings

The definition of a shadow of an ODE system is given by:

**Definition 1.24.** An approximate trajectory  $y = \{y_n\}_{n \in \mathbb{Z}}$  with time steps  $\{h_n\}_{n \in \mathbb{Z}}$  is  $\epsilon$ -shadowed by a true solution if there exists a sequence of points  $x = \{x_n\}_{n \in \mathbb{Z}}$  with time steps  $\{\tau_n\}_{n \in \mathbb{Z}}$  such that  $x_{n+1} = \varphi_{\tau_n}(x_n)$  where  $\varphi_{\Delta t}$  is the  $\Delta t$ -flow of the system, and  $|y_n - x_n| < \epsilon$  and  $|\tau_n - h_n| < \epsilon$ .

Now define the set  $l^\infty(\mathbb{Z}, \mathbb{R}^n)$  as the space of  $\mathbb{R}^n$ -valued bounded sequences  $x = \{x_n\}_{n \in \mathbb{Z}}$  with norm  $\|x\| = \sup_{n \in \mathbb{Z}} |x_n|_2$ , and the set  $C^{1,Lip}(\Omega, \Omega)$  as the ensemble of  $C^1$ -valued Lipschizian functions on  $\Omega \subset \mathbb{R}^n$ . A discrete version of Theorem 1.21 was given with its detailed proof in [Stoffer and Palmer (1999)] by:

**Theorem 1.22.** Let  $\Omega \subset \mathbb{R}^n$  be open,  $f \in C^{1,Lip}(\Omega, \Omega)$  be injective,  $y = \{y_k\}_{k \in \mathbb{Z}} \in \Omega^{\mathbb{Z}}$  be a given sequence, let  $\{A_k\}_{k \in \mathbb{Z}}$  be a bounded sequence of  $k \times k$  matrices, and let  $\delta, \delta_1, m$  be positive constants. Assume that the operator  $L : l^\infty(\mathbb{Z}, \mathbb{R}^n) \rightarrow l^\infty(\mathbb{Z}, \mathbb{R}^n)$ , defined by

$$(Lz)_k = z_{k+1} - A_k z_k, \tag{1.48}$$

is invertible and that

$$\|L^{-1}\| \leq \frac{1}{\delta_1 + \sqrt{2m\delta}}. \tag{1.49}$$

Then the numbers

$$r_0 = \frac{2\delta}{\frac{1}{\|L^{-1}\|} - \delta_1 + \sqrt{\left(\frac{1}{\|L^{-1}\|} - \delta_1\right)^2 - 2m\delta}} \tag{1.50}$$

$$r_1 = \frac{\frac{1}{\|L^{-1}\|} - \delta_1 + \sqrt{\left(\frac{1}{\|L^{-1}\|} - \delta_1\right)^2 - 2m\delta}}{m} \tag{1.51}$$

satisfy  $0 < r_0 \leq r_1$ . Let  $\rho \in [r_0, r_1]$ . Moreover, assume that the set  $\overline{\cup_{n \in \mathbb{Z}} B_\rho(y_n)}$  (the closure) is in  $\Omega$  and that for every  $n \in \mathbb{Z}$

$$|y_{k+1} - f(y_k)| < \delta \tag{1.52}$$

$$|A_k - Df(y_k)| < \delta_1 \tag{1.53}$$

$$|Df(u) - Df(v)| < m|u - v|, u, v \in B_\rho(y_k) \tag{1.54}$$

Then there is a unique  $r_0$ -shadowing-orbit  $x = \{x_k\}_{k \in \mathbb{Z}}$  of  $y$ . Moreover, there is no orbit  $\tilde{x}$  other than  $x$  with

$$|\tilde{x} - y| < \rho. \tag{1.55}$$

Here are three important things to note about the shadow of an orbit:

- (1) The numerical solution is shadowed if it closely follows the path of a true solution.
- (2) The linear growth of errors for the considered system is due to a lack of hyperbolicity in the direction of the flow in phase space [Eric and Vleck (1995)].
- (3) Since the shadowing lemmas used for proving the existence of a shadow require the computation of the Jacobian of the map or solving the variational equations of the ODE's and then estimating hyperbolicity, this method is direct [Palmer (1988), Chow and Palmer (1992)].

This method has been successfully applied to the Hénon map. See Sec. 2.5.6.

### 1.9.2 Homoclinic orbit shadowing

In [Coomes *et al.* (2005)], a new computer-assisted technique with two main components for the rigorous proof of the existence of a transversal homoclinic orbit to a periodic orbit (or a fixed point) of diffeomorphisms in  $\mathbb{R}^n$  is presented. The computation of a suitable pseudo (approximate) homoclinic orbit to a pseudo-periodic orbit was done using the global Newton's method introduced in Sec. 1.3.3.1. Then a homoclinic shadowing theorem (Theorem 1.23, 1.24 given below) is applied to prove the existence of a true transversal homoclinic orbit to a true periodic orbit near these pseudo-orbits of the Hénon map [Hénon (1976)]<sup>14</sup>. See Sec. 2.5.6.

**Theorem 1.23.** (*Connecting Orbit Shadowing Theorem*) Suppose  $f : \mathbb{R}^n \rightarrow \mathbb{R}^n$  is a  $C^2$  diffeomorphism, and  $\{x_k, k \in \mathbb{Z}\}$  to  $\{y_k, k \in \mathbb{Z}\}$  are two  $\epsilon$ -pseudo-periodic-orbits with periods  $N$  and  $N'$ , respectively, of  $f$ . Let  $z = \{z_k, k \in \mathbb{Z}\}$  be an  $\epsilon$ -pseudo-connecting-orbit of  $f$  connecting  $\{x_k, k \in \mathbb{Z}\}$  to  $\{y_k, k \in \mathbb{Z}\}$ . Suppose that the operator  $Lz$  defined in (1.48) is invertible and set

$$\epsilon_z = 2 \|L^{-1}z\| \epsilon \quad (1.56)$$

and

$$M_z = \sup \{ \|D^2 f(u)\| : u \in \mathbb{R}^n, \|u - z_k\| \leq \epsilon_z \text{ for some } k \in \mathbb{Z} \} \quad (1.57)$$

<sup>14</sup>Also, note that it was shown in [Coomes *et al.* (2005)] that all the quantities in the hypotheses of Theorem 1.23, 1.24 are computable.

Then if

$$2M_z \|L^{-1}z\|^2 \epsilon < 1, \quad (1.58)$$

(i) The pseudo-periodic orbits  $\{x_k, k \in \mathbb{Z}\}$  to  $\{y_k, k \in \mathbb{Z}\}$  are  $\epsilon_z$ -shadowed by the unique true hyperbolic periodic orbits  $\{v_k, k \in \mathbb{Z}\}$  of period- $N$  and  $\{w_k, k \in \mathbb{Z}\}$  of period- $N'$ .

(ii) The pseudo-periodic orbit  $\{z_k, k \in \mathbb{Z}\}$  is  $\epsilon_z$ -shadowed by a unique true transversal connecting orbit  $\{e_k, k \in \mathbb{Z}\}$  connecting the true periodic orbit  $\{v_k, k \in \mathbb{Z}\}$  to the periodic orbit  $\{w_k, k \in \mathbb{Z}\}$ . In fact,  $\lim_{k \rightarrow -\infty} \|e_k - u_k\| = 0$ , and  $\lim_{k \rightarrow \infty} \|e_k - v_k\| = 0$ .

**Theorem 1.24.** (Homoclinic Orbit Shadowing Theorem) Suppose  $f : \mathbb{R}^n \rightarrow \mathbb{R}^n$  is a  $C^2$  diffeomorphism and  $\{x_k, k \in \mathbb{Z}\}$  is an  $\epsilon$ -pseudo-periodic-orbit of  $f$  with period- $N$ . Let  $\{z_k, k \in \mathbb{Z}\}$  be an  $\epsilon$ -pseudo-homoclinic-orbit of  $f$  connecting  $\{x_k, k \in \mathbb{Z}\}$  to  $\{y_{k+\tau}, k \in \mathbb{Z}\}$ , where  $0 \leq \tau < N$ . Suppose that the operator  $Lz$  is invertible, and the set

$$\epsilon_z = 2 \|L^{-1}z\| \epsilon \quad (1.59)$$

and

$$M_z = \sup \{ \|D^2 f(u)\| : u \in \mathbb{R}^n, \|u - z_k\| \leq \epsilon_z \text{ for some } k \in \mathbb{Z} \} \quad (1.60)$$

Then if

$$\begin{cases} 2M_z \|L^{-1}z\|^2 \epsilon < 1 \\ \|x_k - x_j\| > 2\epsilon_z, \text{ for } j \neq k, k < N, \end{cases} \quad (1.61)$$

(i) The pseudo-periodic orbit  $\{x_k, k \in \mathbb{Z}\}$  is  $\epsilon_z$ -shadowed by a unique true hyperbolic periodic orbit  $\{v_k, k \in \mathbb{Z}\}$  of minimal period- $N$ .

(ii) The pseudo-homoclinic orbit  $\{z_k, k \in \mathbb{Z}\}$  is  $\epsilon_z$ -shadowed by a unique true orbit  $\{e_k, k \in \mathbb{Z}\}$ . When  $\tau > 0$ , the point  $e_0$  is a transversal homoclinic point to the periodic orbit  $\{v_k, k \in \mathbb{Z}\}$  with phase shift  $\tau$ . When  $\tau = 0$ , the point  $e_0$  is a transversal homoclinic point to the periodic orbit  $\{v_k, k \in \mathbb{Z}\}$  with phase shift 0 provided that  $\|z_k - x_k\| > 2\epsilon_z$  for some  $k$  with  $p < k < q$ .

For the proof of Theorems 1.23, 1.24, two lemmas are required, where the first lemma establishes infinite-time shadowing of a pseudo-orbit by a true hyperbolic orbit without any uniform hyperbolicity requirement for the considered diffeomorphism. The second lemma gives a hyperbolicity-type condition under which two orbits shadowing the same pseudo-orbit must be asymptotic to each other [Coomes *et al.* (2005)]. An example showing how to how apply Theorem 1.23, 1.24 to the Hénon map is given in Sec. 2.6.3.

### 1.10 Method based on the second-derivative test and bounds for Lyapunov exponents

This method based on the *second-derivative test* [Thomas and Finney (1992)] and *bounds for Lyapunov exponents* [Li and Chen (2004)] was introduced first in [Zeraoulia and Sprott (2008a)] for the rigorous proof of the nonexistence and existence of chaos and hyperchaos in the general 2-D quadratic map shown in Chapter 3. We give in this section the definition of the so-called *second-derivative test* and its properties, and we state the theorems determining the upper and lower bounds for the Lyapunov exponents of a discrete mapping.

Let  $h : \mathbb{R}^2 \rightarrow \mathbb{R}$ , be a real function, and assume that  $h$  has continuous partial derivatives at least in the region of interest. The problem of determining the extreme values of a function, i.e., maxima or minima, is encountered in several fields such as geometry, mechanics, physics, as well as the present situation.

**Definition 1.25.** The critical points of the function  $h(x, y)$  are solutions of the equations

$$\frac{\partial h(x, y)}{\partial x} = 0, \frac{\partial h(x, y)}{\partial y} = 0 \quad (1.62)$$

Note that Eqs. (1.62) must be solved simultaneously. However, not all critical points are maxima or minima. For example, the function  $h(x) = x^3$  has critical point at  $x = 0$ , but it is neither a maximum nor a minimum, but rather it is an inflection point.

Let  $(x_c, y_c)$  be a critical point, and define

$$d_h(x_c, y_c) = \frac{\partial^2 h(x, y)}{\partial x^2}(x_c, y_c) \frac{\partial^2 h(x, y)}{\partial y^2}(x_c, y_c) - \left( \frac{\partial^2 h(x, y)}{\partial x \partial y}(x_c, y_c) \right)^2. \quad (1.63)$$

Then we have the following theorem [Thomas and Finney (1992)]:

**Theorem 1.25.** (1) If  $d_h(x_c, y_c) > 0$  and  $\frac{\partial^2 h(x, y)}{\partial x^2}(x_c, y_c) < 0$ , then  $h(x, y)$  has a relative maximum at  $(x_c, y_c)$ .

(2) If  $d_h(x_c, y_c) > 0$  and  $\frac{\partial^2 h(x, y)}{\partial x^2}(x_c, y_c) > 0$ , then  $h(x, y)$  has a relative minimum at  $(x_c, y_c)$ .

(3) If  $d_h(x_c, y_c) < 0$ , then  $h(x, y)$  has a saddle point at  $(x_c, y_c)$ .

(4) If  $d_h(x_c, y_c) = 0$ , then the second-derivative test is inconclusive, and higher order tests must be used.

The second theorem determining the upper and the lower bounds for all the Lyapunov exponents of a given  $n$ -dimensional discrete map was given in [Li and Chen (2004)] by:

**Theorem 1.26.** *If a system  $x_{k+1} = f(x_k)$ ,  $x_k \in \Omega \subset \mathbb{R}^n$ , and*

$$\|Df(x)\| = \|J\| = \sqrt{\lambda_{\max}(J^T J)} \leq N < +\infty, \quad (1.64)$$

*with a smallest eigenvalue of  $J^T J$  that satisfies*

$$\lambda_{\min}(J^T J) \geq \theta > 0, \quad (1.65)$$

*where  $N^2 \geq \theta$ , then for any  $x_0 \in \Omega$ , all the Lyapunov exponents at  $x_0$  are located inside  $[\frac{\ln \theta}{2}, \ln N]$ . That is,*

$$\frac{\ln \theta}{2} \leq l_i(x_0) \leq \ln N, i = 1, 2, \dots, n, \quad (1.66)$$

*where  $l_i(x_0)$  are the Lyapunov exponents for the map  $f$ .*

## 1.11 The Wiener and Hammerstein cascade models

A method based on the Wiener and Hammerstein cascade models [Hunter (1986), Greblicki (1994)] is capable of determining the existence of chaos in dynamical systems. The method uses the following notions of neural networks: The three-layer feed-forward artificial neural network, the non-linear static subsystem, the linear plant, and training of the neural network. Computer simulation given in [Xu *et al.* (2001)] confirms the effectiveness of this method when applied to the Hénon map [Hénon (1976)]. The basic idea of the method is to determine the parameters of the ANN by a model-reference adaptive control scheme using the available outputs of the underlying chaotic system whose formulation may be unknown.

### 1.11.1 Algorithm based on the Wiener model

The architecture of the Wiener model is shown in Fig. 1.6(a), and the structure of the ANN within the Wiener model that is used for the simulation is shown in Fig. 1.8.

If:

$HN$  is the number of hidden units,

$z_{i,j}$  is the weight of the connection from the  $i^{th}$  input unit to the  $j^{th}$  hidden node,

$\omega_j$  is the weight on the connection from the  $j^{\text{th}}$  hidden node to the output,

$h$  is the output of the linear plant (with time delay),

$x(k)$  and  $y(k)$  are the outputs of the plant and the chaotic system, respectively,

$\theta$  is either  $\omega_i$  or  $z_{i,j}$ ,

$\rho$  is the learning rate parameter,

$\eta$  is a dynamical factor,

then the algorithm based on the Wiener model is as follows:

**Algorithm 1.2.** (1) Choose a simple and completely controllable linear plant<sup>15</sup>.

(2) Choose a static nonlinear subsystem<sup>16</sup>.

(3) Calculate the following quantities:

$$\left\{ \begin{array}{l} x = \sum_{j=1}^{HN} \omega_j r_j \\ r_j = f \left( \sum_{i=0}^{n+1} z_{i,j} v_i \right) \\ v_i = \begin{cases} h(k-i), & i = 0, \dots, n \\ -1.0, & i = n+1 \end{cases} \end{array} \right. \quad (1.67)$$

(4) Train the ANN by a model-reference adaptive control method using the framework shown in Fig. 1.9(a).

(5) Update the weights of the ANN by minimizing the following least-squares matching measure:

$$\bar{J} = \frac{1}{2} (y(k) - x(k))^2 \quad (1.68)$$

<sup>15</sup>This plant can be in the first canonical form, with the same dimension as the unknown chaotic system to be identified. If the dimension of the chaotic system is unknown, then it is possible to increase the dimension during the training process until satisfactory results are obtained.

<sup>16</sup>Generally, one can use a simple three-layer feed-forward ANN with the sigmoidal function  $f(x) = \frac{1}{1+e^{-x}}$  and a linear activation function for the hidden and output layer neurons, respectively. Fig. 1.8 shows that the inputs of the ANN are the signals from the plant outputs with a time delay, and the outputs of the ANN are trained to synchronize to the given chaotic system.

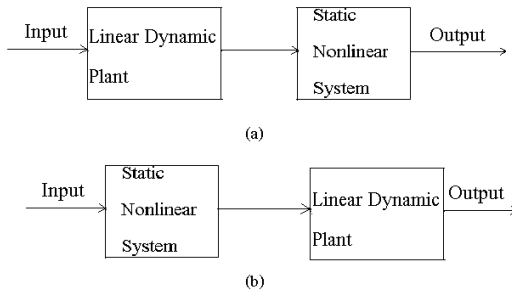


Fig. 1.6 (a) The Wiener model. (b) The Hammerstein model.

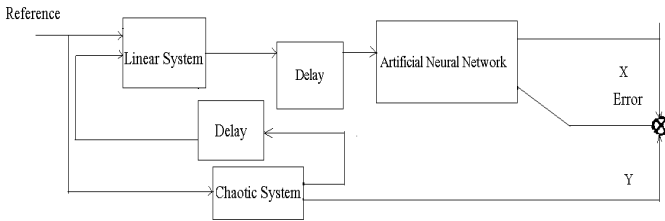


Fig. 1.7 The learning mechanism of the Wiener model.

according to the following equations:

$$\left\{ \begin{array}{l} \theta = \theta + \rho(k) [(1 - \eta) D(k) + \eta D(k - 1)] \\ \rho(k) = 2^\lambda \rho(k - 1) \\ \lambda = \text{sgn}[D(k) D(k - 1)] \\ D(k) = -\Delta(k) \frac{\partial x(k)}{\partial \theta} \\ \Delta(k) = y(k) - x(k) \\ \frac{\partial x(k)}{\partial \theta} = \begin{cases} r_j, & \text{if } \theta \text{ is } \omega_j \\ \omega_j r_j (1 - r_j) v_i, & \text{if } \theta \text{ is } z_{i,j}, j = 1, HN \\ v_i = \begin{cases} h(k - i), & i = 0, \dots, n \\ -1.0, & i = n + 1 \end{cases} \end{cases} \end{array} \right. \quad (1.69)$$

(6) If an error at the output layer is obtained, then it can be propagated backwards to update the weight of the hidden layers.

An example of how to apply an algorithm based on the Wiener model to the Hénon map is discussed in Sec. 2.5.4.

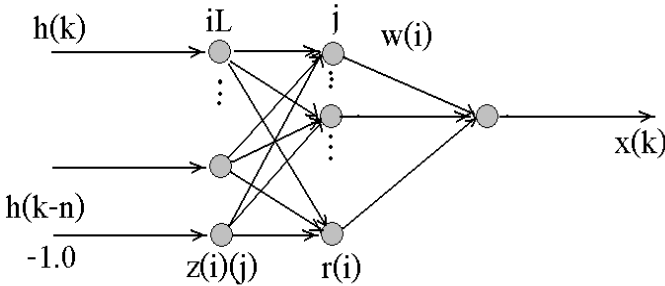


Fig. 1.8 The three-layer feed-forward ANN.

1.11.2 Algorithm based on the Hammerstein model

The architecture of the Hammerstein model is shown in Fig. 1.9(b). Similar to the Wiener model, a simple linear plant is chosen to be completely controllable and to have the same dimension as the given chaotic system, and a simple three-layer feed-forward ANN is used to approximate the static nonlinearity, which is the same as that shown in Fig. 1.8. Again the inputs of this ANN are the feedback signals from the chaotic system outputs with time delay. Suppose the linear subsystem of the Hammerstein model can be represented as:

$$x(k) = \sum_{i=1}^n a_i x(k-i) + u(k-1). \tag{1.70}$$

The algorithm based on the Hammerstein model is as follows:

**Algorithm 1.3.** (1) Choose a simple and completely controllable linear plant.

(2) Choose a static nonlinear subsystem.

(3) Calculate the following quantities:

$$\left\{ \begin{array}{l} x(k) = \sum_{i=1}^n a_i x(k-i) + u(k-1) \\ x = \sum_{j=1}^{HN} \omega_j r_j \\ r_j = f\left(\sum_{i=0}^{n+1} z_{i,j} v_i\right) \\ v_i = \begin{cases} h(k-i), & i = 0, \dots, n \\ -1.0, & i = n+1 \end{cases} \end{array} \right. \tag{1.71}$$

(4) Train the ANN by a model-reference adaptive control method through the framework shown in Fig. 1.8.

(5) Update the weights of the ANN by minimizing the following least-squares matching measure:

$$\bar{J} = \frac{1}{2} (y(k) - x(k))^2 \quad (1.72)$$

according to the following equations:

$$\left\{ \begin{array}{l} \theta = \theta - \rho \Delta(k) \eta(k) \\ \Delta(k) = x(k) - y(k) \\ \eta(k) = \sum_{i=1}^n a_i \eta(k-i) + \frac{\partial u(k-1)}{\partial \theta} \\ \frac{\partial u}{\partial \theta} = \begin{cases} r_j, & \text{if } \theta \text{ is } \omega_j \\ \omega_j r_j (1 - r_j) v_i, & \text{if } \theta \text{ is } z_{i,j} \end{cases}, j = 1, HN \\ v_i = \begin{cases} h(k-i), & i = 0, \dots, n \\ -1.0, & i = n+1 \end{cases} \end{array} \right. \quad (1.73)$$

(6) If an error at the output layer is obtained, then it can be propagated backwards to update the weight of the hidden layers.

An example of how apply an algorithm based on the Hammerstein model to the Hénon map is discussed in Sec. 2.5.4.

## 1.12 Methods based on time series analysis

An example of these methods is given in [Bhattacharya and Kanjilal (1999)] where the nonlinearly scaled distributions of the strengths of the orthogonal modes in the data of a time series are compared with those derived from its surrogate counterpart to assess its chaoticity, which manifests itself in the decreasing strengths of the weaker modes with increasing dimension of the orthogonal spaces mapping the process. This method is applied to the Hénon map in Sec. 2.5.5 where some criteria are used to distinguish chaos from other dynamical behaviors based on the fact that the chaotic process has a finite number of modes compared to the infinitely large number of modes in its stochastic counterpart.

Let  $\{x(k)\} = \{x(1), x(2), \dots\}$  be the series in question. The series  $\{x(k)\}$  is configured into matrices with different row lengths  $n$  for analysis using singular value decomposition (SVD)<sup>17</sup>. In each case, successive  $n$ -long segments of the series are arranged into successive rows of the  $m \times n$  matrix  $A$ , and  $A$  is singular-value decomposed. The quantity  $n$  is varied over a

<sup>17</sup>Singular value decomposition (SVD) is a factorization in the form of the product of a rectangular real or complex matrix.

wide range to capture the embedded dynamics in  $\{x(k)\}$ . The matrix  $A$  with any dimension  $m \times n$  is given by:

$$A = \begin{pmatrix} x(1) & x(2) & x(3) & \dots & x(n) \\ x(n+1) & x(n+2) & x(n+3) & \dots & x(2n) \\ \dots & \dots & \dots & \dots & \dots \\ x(1+n(m-1)) & x(2+n(m-1)) & \dots & \dots & x(nm) \end{pmatrix} \quad (1.74)$$

Before the algorithm for this method is given and discussed, we need the following results [Golub and VanLoan (1989), Kanjilal (1995)]:

**Definition 1.26.** Singular value decomposition of an  $m \times n$  matrix  $A$  is given by  $A = U\Sigma V^T$  where  $U = [u_1, \dots, u_m] \in \mathbb{R}^{m \times m}$  and  $V = [v_1, \dots, v_n] \in \mathbb{R}^{n \times n}$  are orthogonal matrices such that

$$U^T AV = \Sigma = [\text{diag}[\sigma_1, \dots, \sigma_p] : 0] \in \mathbb{R}^{m \times n}, \quad (1.75)$$

where  $p = \min(m; n)$ , and  $\sigma_1 \geq \sigma_2 \geq \dots \geq \sigma_p \geq 0$  are the singular values of  $A$  which are non-negative.  $U$  and  $V$  are the left and the right singular vector matrices, respectively. The decomposed conjugate vector pairs  $u_1$  and  $v_1$  have related physical meaning [Good (1969), Golub and VanLoan (1989), Kanjilal (1995)].

**Theorem 1.27.** (a) *The left and right singular vectors form a basis for the row-space and the column-space of  $A$ , respectively.*

(b) *The singular values of  $A$  are the positive square roots of the eigenvalues of  $A^T A$  or  $AA^T$ .*

(c) *The number of nonzero singular values gives the rank of the matrix  $A$ .*

The matrix configuration  $A$  given by Eq. (1.74) offers some inherent advantages in characterization of the time-series  $\{x(k)\}$ : Indeed,

**Lemma 1.8.** (a) *If the series  $\{x(k)\}$  is nearly periodic with a repeating periodic pattern having periodicity  $n$ , then the  $m \times n$  matrix  $A$  has nearly rank one because  $\sigma_1 \gg \sigma_2$ .*

(b) *If the series  $\{x(k)\}$  is truly random, then  $A$  has the full rank with the singular values having comparable magnitudes.*

In the case where  $\{x(k)\}$  is nearly periodic, the vector  $v_1$  gives the pattern over periodic segments, and the elements of  $u_1$  give the scaling factors for the successive periodic segments [Kanjilal (1995)].

Hence the distinguishing features between deterministic and nondeterministic processes are expected to be reflected in the distribution of the nonprime singular values.

The proposed algorithm [Bhattacharya and Kanjilal (1999)] is as follows:

**Algorithm 1.4.** (1) Generate a surrogate series  $\{x_{surr}(k)\}$  from the given series  $\{x(k)\}$  such that  $\{x_{surr}(k)\}$  is the nondeterministic counterpart of  $\{x(k)\}$ <sup>18</sup>. (2) Find the different configurations of  $m \times n$  matrices  $A$  and  $A_{surr}$  from  $\{x(k)\}$  and  $\{x_{surr}(k)\}$ .

(3) Generate and analyze the scaled distributions of the respective singular values as follows:

(3-1) Normalize the total energy in  $A = (a_{ij})$  given by

$$Q_A = \sum_i \sum_j a_{ij}^2 = \sum_i \sigma_i^2 \quad (1.76)$$

for each configuration  $A$ , preserving the Frobenius norm (where  $\|A\|_F = Q_A$ ) of  $A$ .

(3-2) Choose a value<sup>19</sup>  $R$  close (which is not a limitation) to the minimum value of the maximum rank<sup>20</sup>  $p$ .

(3-3) Calculate the mean singular values<sup>21</sup>  $\sigma_m(i)$ ,  $i = 1, R$ .

(3-4) Plot the scaled distribution  $i^2 \sigma_m(i)$  versus  $i$  for  $i = 1, R$  for both  $\{x(k)\}$  and  $\{x_{surr}(k)\}$  allowing for the detection of determinism in  $\{x(k)\}$ .

First, for a purely stochastic series  $\{x(k)\}$ , all the singular values are isotropically distributed, and the scaled distribution  $i^2 \sigma_m(i)$  will gradually increase, tending to saturate at a high value since the singular values are arranged in a nonincreasing order. Second, for a chaotic series with increasing  $i$ , the singular values  $\sigma_i$  will have significantly decreasing magnitudes, tending to become vanishingly small, and hence the scaled distribution  $i^2 \sigma_m(i)$  will eventually decrease, tending to saturate asymptotically at a low value. The distribution of  $i^2 \sigma_m(i)$  versus  $i = 1, R$  for  $\{x(k)\}$  and  $\{x_{surr}(k)\}$  are compared using the Mann-Whitney (M-W) rank-sum statistic  $(Z)^2$  [Zar (1984)], which is a nonparametric test for assessing whether two samples of observations come from the same distribution. The null hypothesis is that the two samples are drawn from a single population and therefore that their

<sup>18</sup>The *unwindowed amplitude adjusted Fourier transform* (AAFT) surrogate generator [Theiler *et al.* (1992), Kennel and Isabelle (1992)] can be used to generate  $\{x_{surr}(k)\}$ .

<sup>19</sup>For each configuration of  $A$ , the total energy  $Q_A$  is linearly mapped to  $R$  normalized singular values; thus the normalized energy is conserved.

<sup>20</sup>Since the maximum rank  $p$  is different for different configurations of  $A$ .

<sup>21</sup> $M$  different values of row length  $n$ , and  $M$  sets of  $R$  singular values are obtained.

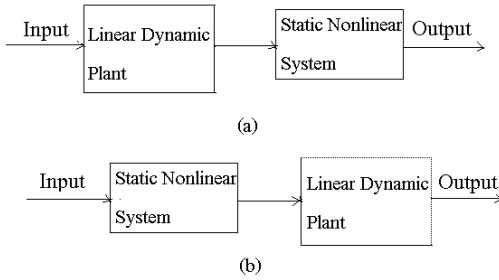


Fig. 1.9 (a) The learning mechanism of the Wiener model. (b) The learning mechanism of the Hammerstein model.

probability distributions are equal. Consider two distributions, namely  $B$  and  $D$  with length  $N_1$  and  $N_2$ , respectively; compute  $U$  as

$$W = \sum_{i=1}^{N_1} \sum_{j=1}^{N_2} \chi(B_i - D_j) \tag{1.77}$$

where  $\chi$  is a Heaviside function (i.e.,  $\chi(x) = 1$  for  $x > 0$ , and  $\chi(x) = 0$  for  $x \leq 0$ ). For large  $N_2$  (which in practical terms means a few tens), the Mann-Whitney (M-W) rank-sum statistic is given by

$$Z = \frac{W - \frac{1}{2}N_1N_2}{\sqrt{\frac{1}{12}N_1N_2(N_1 + N_2 + 1)}}. \tag{1.78}$$

Hence one has the following result:

**Theorem 1.28.** *The Mann–Whitney rank-sum statistic  $Z$  is normally distributed with zero mean and unit variance under the null hypothesis that the two observed samples came from the same distribution.*

Then if we observe a  $|Z|$  value greater than 1.96 [Zar (1984)], we can reject the null hypothesis at the 95% confidence level.

An example to how to apply the algorithm based on time series analysis to the Hénon map is given in Sec. 2.5.5.

### 1.13 A new chaos detector

The term ‘chaos detector’ was introduced in [McDonough *et al.* (1995)], and it denotes a new criterion for detecting chaos in dynamical systems just like

the largest Lyapunov exponent and the different types of dimensions and entropies defined for dynamical systems. An example of its application to the Hénon map is given in Sec. 2.5.8. The main ideas of this method include the search for short periodic sequences, the mean squared errors, and a two-point reference set  $\{0, 1\}$ . Chaotic behavior is indicated by the presence of sharp isolated peaks in the resulting histogram. Note that this method has the following advantages:

- (1) It is simpler, numerically less intensive, and more robust than previous methods.
- (2) It works well with short data sets and with severe data quantization even in the presence of noise.

The algorithm for this method is called **MESAH** because it uses the so-called *MEan SquAred error histogram*, and is given by the following:

- (1) Begin with a data set<sup>22</sup>  $x(i), i = 1, 2, \dots, N$ .
- (2) Let  $x_{\max} = \max \{x(i), i = 1, 2, \dots, N\}$ .
- (3) Let  $x_{\min} = \min \{x(i), i = 1, 2, \dots, N\}$ .
- (4) For  $i = 1$  to  $N - 1$

$$\text{value}(i) = \frac{1}{2} \left[ (x(i) - x_{\max})^2 + (x(i+1) - x_{\min})^2 \right]. \quad (1.79)$$

- (5) Plot a histogram of the value array<sup>23</sup>.

## 1.14 Exercises

- (1) (a) Find the equilibrium points of the system (1.1) modelling a three-dimensional Smale-Williams attractor.
  - (b) Determine the corresponding stable and unstable manifolds for each equilibrium point.
  - (c) Choose an appropriate Poincaré section  $S$ , and draw the corresponding bifurcation diagram for a chosen set of parameters showing a route to chaos.
  - (d) Search for a hyperchaotic attractor.
  - (e) Compare the behavior of Eq. (1.1) with the original Smale-Williams attractor.

<sup>22</sup> $x(i)$  here is a component of a map.

<sup>23</sup>This is the *MESAH array* of the scaled squared distances in  $\mathbb{R}^2$ , i.e.,  $x(i+1)$  versus  $x(i)$  which gives an attractor in the sense of dynamical systems.

- (2) Derive the relation (1.14).
- (3) Derive the Mean value form of Theorem 1.2.
- (4) Prove Lemma 1.1 and Lemma 1.2.
- (5) Show that the image of the vertical edges defined in (1.19) does not intersect the set  $N$  given in (1.20) and that the image of  $N$  is contained in the set which can be continuously deformed to the horizontal strip without any intersection with the horizontal edges of  $N$ .
- (6) Prove Lemmas 1.3, 1.4 and 1.6(a).
- (7) Prove Lemma 1.7 using the geometrical formation of Smale's horseshoe map  $f$ .
- (8)
  - (1) Draw all the sets included in the definition of the map (1.36).
  - (2) Find the images of the sets  $\tilde{N}_0$  and  $\tilde{N}_1$ .
  - (3) Find the fixed points of the map (1.36).
  - (4) Using the linearity of the horseshoe map, show that for every  $n \in \mathbb{N}$  there is still a period- $n$  point  $(u, v)$  of the map (1.36).
  - (5) Show that the Jacobian of  $f^n$  is given by (1.37).
  - (6) Show that there exists a neighborhood  $U$  of the point  $(u, v)$  which does not contain other fixed points of  $f^n$ .
  - (7) Calculate the fixed point index of the pair  $(f^n, U)$ , and deduce that there are  $2^n$  fixed points of the map  $f^n$ .
- (9) Prove Theorem 1.5 and 1.7.
- (10) Find a piecewise linear version of the heteroclinic Theorem 1.12.
- (11) Find bounds for Lyapunov exponents of the Hénon map using Theorem 1.26 for  $a = 1.4$  and  $b = 0.3$ .
- (12) Show the algebraic Theorem 1.27.